UNIVERSITY OF CALABRIA CHEMISTRY DEPARTMENT

A DFT AND TDDFT STUDY OF MOLECULES WITH INTEREST ON PHOTODYNAMIC THERAPHY

Flavio Fortes Ramos Sousa

Rende, 2012

Table of contents

1) SUMMARY

This PhD work concerns the theoretical photochemistry study of molecules with an interest on Photodynamic Therapy (PDT). PDT is a medical technique for the treatment of different tumor diseases, such as age related macular degeneration, psoriasis or bladder cancer. This technique is increasingly being required, in particular in cases when conventional methods, chemotherapy and radio therapy fail to be successful.

It consists of the administration of photosensitizer (a drug) followed by light irradiation and requires the presence of molecular oxygen on tissue to be destructed. On molecular terms the action of the drug is explained by the excitation of the drug to a singlet state after light irradiation, followed by its conversion of to a triplet state.

This triplet state, in more common cases, directly transfers its energy to molecular oxygen producing singlet oxygen. In other cases the photophysical parameters of the triplet state are such that it is allowed to participate in electron transfer reactions, where it becomes reduced and after its anion reduces oxygen forming radical oxygen species, that like singlet oxygen, is toxic to the cell, resulting in cellular death by apoptosis or necrosis.

As chemists, our main interest is on the proposal of drugs with ideal photophysical and solution properties. In regards to the first aspect, a drug should have an intense absorption on the red part of the visible spectra, known as therapeutic window, where the body tissue has a better penetration.
Furthermore, the drug should have ideal photochemistry parameters to participate in the reaction. For the activation of oxygen it should have a triplet energy higher than the 0.98 eV of oxygen triplet and for others photochemical mechanism of action it should have the ideal parameters namely, ionization potentials and electron affinities.

The drug should be soluble in water to react on the cells, that is usually provided by an hydrophilic chemical group incorporated on the drug. In order to have fewer side effects and a decreased drug dose, the drug should preferentially be localized on the tumor site.

In reality, the question to find an ideal drug goes beyond chemistry crossing the fields of physics and clinical medicine. It involves physical problems like the interaction of light and body tissue with better

dispositive or lasers for light irradiation to be developed. On the clinical part, it is evaluated on the in vitro or in vivo toxicity of the drug as well as the drug's side effects.

The organic and inorganic chemists are interested on the synthesis and characterization of the new drugs.

The developments of new quantum mechanics methods with a good balance between accuracy and computational cost, namely Density Functional Theory (DFT) allowed the theoretical chemists to contribute to diverse fields like bio-medicine and other fields where the size of the systems can have dimensions large enough to be studied by older quantum mechanics methods.

On the particular question of PDT, the simulation of electronic spectrum and calculation of photochemical parameters can be a support to the work of experimentalist on his synthesis strategy and on the interpretation of obtained data.

The chemist experimental work on PDT, usually starts with a tetrapyrrolic macrocycle, natural like porphyrin or synthetic like phthalocyanine. Its structure is modified by the incorporation of substituent groups (e.g phenyl groups) that extends the electron conjugation that can shift the maximum absorption wavelength, $\lambda_{max,}$ to red part.

The possibility of predicting the effect of a substituent group can address the synthesis to a molecule than another. Also, the calculation of the photochemical parameters of the drug allows the evaluation of the feasibility of a mechanism. For example, the electronic energy of the first triplet state furnishes a first estimation on the capability of a drug to generate singlet oxygen.

The theoretical methodology in this work is Density Functional Theory (DFT) for the optimization of the structures and its time dependent formalism (TDDFT) for the calculation of electronic excitations. The behavior in solutions is simulated by the solvent implicit methods(C-PCM).

On the first part of the study, we focus on two compounds designed to be used on PDT, belonging to the class pentaporphyrins that are porphyrin like molecules containing five pyrrole rings. These compounds were subject to clinical studies were they have shown a PDT action. We predict the electronic spectra and further investigate the mechanism of action of these compounds.

On a second part of the study, we focus on corroles - molecules analogues to porphyrin - and its metal complexes, which synthesis were recently reported. We investigate the electronic spectra and evaluate the ability to produce singlet oxygen.

The third part of the study consists on a non porphyrin based compounds – the squarines. These molecules are much known to their use in photo cells devices. Their sharp transitions make them as promising drugs to be used on PDT.

2) INTRODUCTION

Tumor Photodynamic therapy

Historical introduction and general aspects

The therapeutic effect of solar light on the human body, known as heliotherapy, has been used since the antiquity by Greeks like Erodoto (VI sec. B.C) who reported the beneficial effects of the solar light on the bone development and Ippocrate (460-375 B.C) who defended the use of solar light for the cure of several diseases. These empirical observations were confronted by the scientific methods at the end of 19 th century by Niel Rydberg Finsen, a physician born at 1860 on the Farao islands that worked on Copenhagen. Finsen conducted his experiments noticing the effects caused by radiation of diverse colors on animals and in particular proposed the use of pink radiation to improve the recuperation and cicatrization in patients affected by smallpox. However his greatest contribution concern the treatment and cure of a cutaneous form of tuberculosis (*Lupus vulgaris*) that was much diffused during that time on the north countries. The technique consisted on the use of the light generated by a carbonic arch lamp filtered by water or quartz to reduce the infrared intensity on parts of the body to be treated. This research culminated with the assignment of the Nobel Prize of Physiology and Medicine to the author in 1903, one year before his death and was brought to the foundation of the research institute (Medical Light Institute) in honour of him. Over the successive years, this technique was also adopted on United Kingdom in which Royal London Hospital was inaugurated a Light Department showing the attention of the field on those days. With time the interest in phototherapy has declined progressively because of unclear reasons, such as the decrease spread of *Lupus vulgaris* or the excessive optimism put on the general utilization of the therapy.

However, over the recent decades, a wave of interest reappeared on the therapeutic use of the light because of several discoveries. One important discovery was the synthesis of Vitamin D on the human skin.Vitamin D is a crucial vitamin for the regulation of calcium and phosphorous level on the blood. Its deficiency is related to many diseases like osteoporosis, bone fracture and others. The first step in its synthesis is the conversion of 7-Dehydrocholesterol to pre-vitamin D, a reaction that requires light on the ultraviolet B region (290-315 nm). This case of phototherapy belongs to the category of Direct Phototherapy since it requires only the exposure to light without administration of a drug. The process

starts with the absorption of a photon by a molecule (chromophore) already in the body, exciting the molecule, and therefore promoting a photochemical reaction that was not possible before.

Another important discovery is related to the treatment of psoriasis, a skin disease. On this treatment a drug of psolaren family named 8-MOP (figure 1) is administered to the patient followed by irradiation on the UVA region (320-400 nm). This methodology was initiated on 1953 by Lerner, Denton e Fitzpatrick for the cure of vitiligo, a skin disease with the loss of pigmentation, and developed on 1974 on a research group of Paris. This treatment is indicated by the acronimous PUVA, meaning Psoralen + UVA.

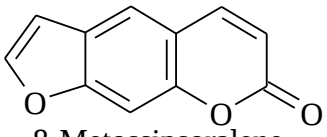

8-Metossipsoralene
(8-MOP)

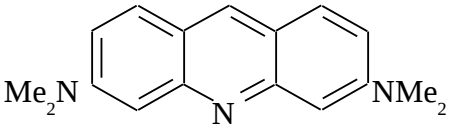

Acridina arancione

Figura 1

This therapy belongs to the category of Indirect Phototherapy or Photochemiotherapy which consists on the administration of a drug followed by light exposure. Phododynamic Therapy, PDT, belongs to this category. However, PDT distinguishes itself since its mechanism of action requires molecular oxygen. The first experiments which have evidenced the photodynamic activity on the destruction of alive tissue were done on 1897-1898 by Oscar Raab, a medical student of Professor H. von Tappeiner at the University of Monaco *Ludwig-Maximilian.* Raab observed that the synergistic action of light and a coloured substance (acridine orange) at low concentrations induced the death of the unicellular organism, paramecium while with the absence of ligh, he did not notice the effect on the paramecium. This discovery stimulated successive research on the field. On 1904, von Tappeiner and Jodlbauer used in vivo the solar radiation to activate the photo sensitive molecule eosin on tumoral tissue. The expression *photodynamic effect* was used for the first time suggesting how the presence of molecular oxygen was necessary for the process. Hasselbach at 1909, using it as a model for the hemolysis of erythrocytes, showed that the photosensitizer agent increased the hemolysis rate only in the the presence of molecular oxygen, confirming the conclusions of von Tappeinevr e al.

The Hans Ficher research laboratory of Organic Chemistry, at Monaco Baviera (1912), registered a strong photodynamic effect on rats which were injected by a subcutaneous way with a solution of hematoporphyrin, a derivative of phorphyrin (figura 2) while with the given same condition,

mesoporphyrin showed no effect.

The first experiment on the human body was done by Friedrich Meyer-Betz, a student of Hans Ficher at October of 1912. Meyer-Betz injected himself intravenously a physiological saline solution of hematoporphyrin and exposed himself to solar light. After two days, there was the appearance of erythema on his skin that only started disappearing after a week while the cutaneous photosensibility remained until the incoming spring. The experiment clearly showed the photodynamic effect of the porphyrin like molecules although they were already known for the action mechanism of some porphyria disease. On porphyria the irregular working of the ferrochelatase enzyme induces an accumulation of free porphyrin on the plasma which, by circulation, reaches the epidermis causing photosensibility especially on the parts more exposed to sun (hands and eyes).

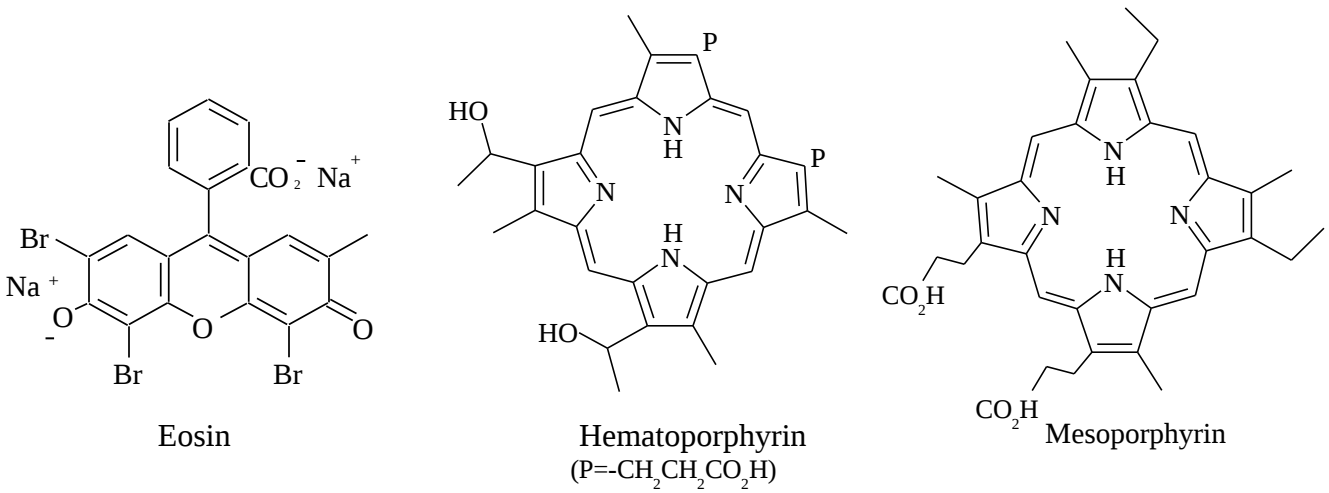

Figura 2

In 1920, Policard noticed that the tumor tissues were more fluorescent than the healthy part and suggested the possibility of using molecules with fluorescence to define better the localization of the tumors. This study of fluorescence became much related to PDT.

Between the years 1940-1960, there have been some experiments conducted by Figge et al. and E Rasmussen et al, consisting on the administration of natural porphyrin to animal and human patients with the intention of localizing tumor tissues accurately, by the fluorescence process, the tumoral tissue. Wilkinson (1960) used tetraphenyl porphyrin with the same goal.

In the early 60’s there was a then wave of interest on Photodynamic Therapy thanks to the work of Lipson and Schwartz. Schwartz used a preparation of hematoporphyrin and after a solution of derivatives of hematoporphyrin to localize a tumor. Lipson, on using hematoporphyrin as a tumor marker, discovered the property of the hematoporphyrin to destruct the tumor tissues.

An important step on the PDT history was taken when Dougherty discovered that the molecule Fluorescein diacetate had cytotoxic activity against the cell TA-3 and could be used as photosensitizer. However the production of a singlet oxygen, already identified as the responsible factor on PDT, was very low for fluorescein. Also, the need to use drugs absorbing on regions close to infrared was pointed out, since this part of the electromagnetic spectra is where maximum penetration of the light is. The fluorescein absorbed more on the green regions and was inadequate to be used since its low penetration on the tissue would require a high dose administration.

The hematoporphyrin derivatives of Schwartz were rediscovered regarding a higher singlet oxygen quantum yield, a absorption maximum band on red part of the spectra and a preferential localization on the tumor cells. The attempt of Dougherty on isolating the active molecules of the hematoporphyrin preparation resulted to the production of a purified drug labeled with the commercial name Photofrin ®. The use of this drug was approved in Canada in 1993 on the treatment of vesicular cancer and with the successive years in Japan, Unites States and some European countries, for the treatment of several tumors like the on the initial and final stages of lung and esophageal cancer.

Despite Photofrin ® belonging to the first generation of PDT agent, it is not an ideal PDT drug considering that it has some collateral effects. For this reason, the scientific research on this field is still very active, bringing to the synthesis of new drugs.

Photochemical processes on Photodynamic therapy

In this section we introduce the principal concepts and terminology related to the interaction of light with molecules. We shall then introduce the properties of molecular oxygen followed by the molecular mechanisms on the process of PDT.

Absorption electronic spectroscopy

The photodynamic action of a molecule is explained on the presence of visible light or electromagnetic light in general, that in classical physics is described as a wave on the space of electric and magnetic

fields mutually perpendicular, to which is associated a wavelength λ, normally expressed in nanometers (nm). The wave character is used on the interpretation of phenomenon like diffraction, refraction and polarization while the corpuscular nature of the radiation is used to understand absorption and emission of light by matter.

On the electromagnetic spectra (figure 3), the visible radiation occupies only a small part that extends from 400(violet) to 750 nm (red). The ultraviolet region divides in UVA, UVB and UVC. The UVA part like the visible light it is important on the study of photobiological processes. The UVB and UVC parts are far more energetic, causing diseases like skin cancer because of the absorption by DNA and some amino acids and for this reason this part of the spectra is not used for medical purposes.

Figure 3

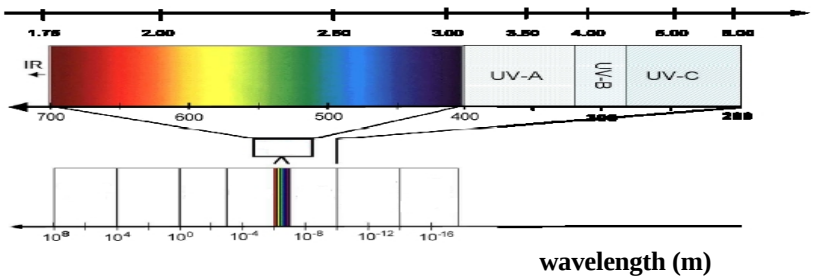

The corpuscular interpretation of the radiation is based on the quantization principle of Max Planck hypothesis (1901) by which the variation in energy on the processes of emission or absorption comes in discrete units of the photon which have the energy:

$$E = h\nu = hc/\lambda$$

Where h is the Planck constant, ν is the frequency of the radiation and c the light velocity.

The absorption of the visible or ultraviolet light induces an electronic transition between the energetic levels of the atoms or molecules. The mechanism can be understood like this:

A molecule at ground state absorbs a photon of incident radiation that induces the transition of an electron to a level of higher energy. On the organic systems the absorption of a photon induces the transition from an bonding orbital of the type π to an anti-bonding orbital of the type π^* ($\pi \rightarrow \pi^*$) or also

from a localized orbital to an π^* ($n \rightarrow \pi^*$).

The ground state of organic molecule with closed shell (all the electrons paired) is a singlet labelled by S_0. Since all the electrons are paired the total spin is zero (S=0) and the multiplicity (2S+1) is one.

The excitation of an electron to the next orbital generates a excited Singlet S_1 when the electrons stay with opposite spins or a triplet state T_1 when the two electrons have opposite spins (figure 4).

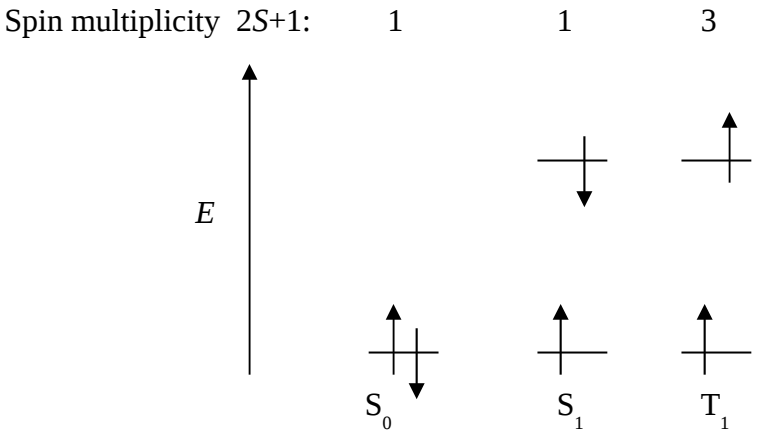

Figura 4

The allowed electronic transitions between the energetic states are deduced from quantum mechanics, in particular from the Time Dependent Perturbative method, in which the electric field of incident electromagnetic wave is represented by a perturbative operator. The transition probability from a initial state i to final state f is proportional to the square of the absolute value of the transition moment Q:

$$P_{if}=|Q|^2=(\langle \psi_i |er| \psi_f \rangle \langle \psi_i^{spin} | \psi_f^{spin} \rangle)^2$$

ψ_i and ψ_f are the spacial initial and final orbitals, er the dipolar moment, ψ_i^{spin} and ψ_f^{spin} the spin initial and final orbitals.

A transition in allowed if $P_{if} \neq 0$, meaning that both factors are different from zero. The dominant rule concerns the spin factor: the transitions are possible only for states with the same multiplicity, for example $S_0 \rightarrow S_1$, since otherwise the spin factor is zero. To this rule constitute an exception the heavy atomic systems (Atomic number > 30).

For the allowed transitions the ones with the higher spacial overlapping are more intense, what explains the greater intensity to the transition $\pi \rightarrow \pi^*$ relative to $n \rightarrow \pi^*$ transition.

On the experimental point of view, on the phenomenon of absorption, the absorbance A, quantifying how much the light is absorbed comes defined as

$$A = \log(I_0/I)$$

I_0 and I are the intensities of the incident and transmitted light. The absorbance, for diluted solutions, is given by the Beer Lambert Law:

$$A = \varepsilon \cdot C \cdot l$$

ε is the molar extinction coefficient, an intrinsic property of the molecule on the respective solvent depends of the wavelength of the incident radiation, C is the concentration of the molecule and l is the distance the light travels through the material.
To express the intensity of a transition we use the oscillator strength, f,

$$f = 4.33 \cdot 10^{-9} \int \varepsilon(\nu) d\nu$$

The integration is because a transition is not associated to a specific value of λ corresponding to difference in energy between the states but by a function with center on this λ what is reflecting the fact that an electronic transition is usually followed up by ro-vibrational transitions.
For allowed transition f is 1 while for forbidden it is << 1. Table 1 shows the relation between f and ε

Table 1

	ε (M^{-1} cm^{-1})	f
Forbidden by spin condition	10^{-5}-10^{0}	10^{-5}
Forbidden by sapcial condition	10^{0}-10^{3}	10^{-1}
Allowed	10^{3}-10^{5}	1

Jablowsky Diagram

Until now we have considered the process of energetic electron promotion from the fundamental, which is the most populated state at room temperature, to the next singlet or triplet excited state. What can happen to the electron after occupying the excited state ? The electron can:

-decay from the singlet or triplet sate to the ground state emitting a photon originating the phenomenon of fluorescence or phosphorescence respectively.

-pass to another state of the same multiplicity, a process named by Internal Conversion IC, a non radiative process that involves the overlapping between the excited state and an excited vibrational of the next sate.

-promote a chemical reaction, for example photocyclization reaction

-transfer its excitation energy to another molecule in a non radiative process, named energy tranfer

-pass to the another state of the different multiplicity, a non radiative process named intersystem spin-crossing isc.

These processes are summarized on the Jablowsky Diagram (figure 5).

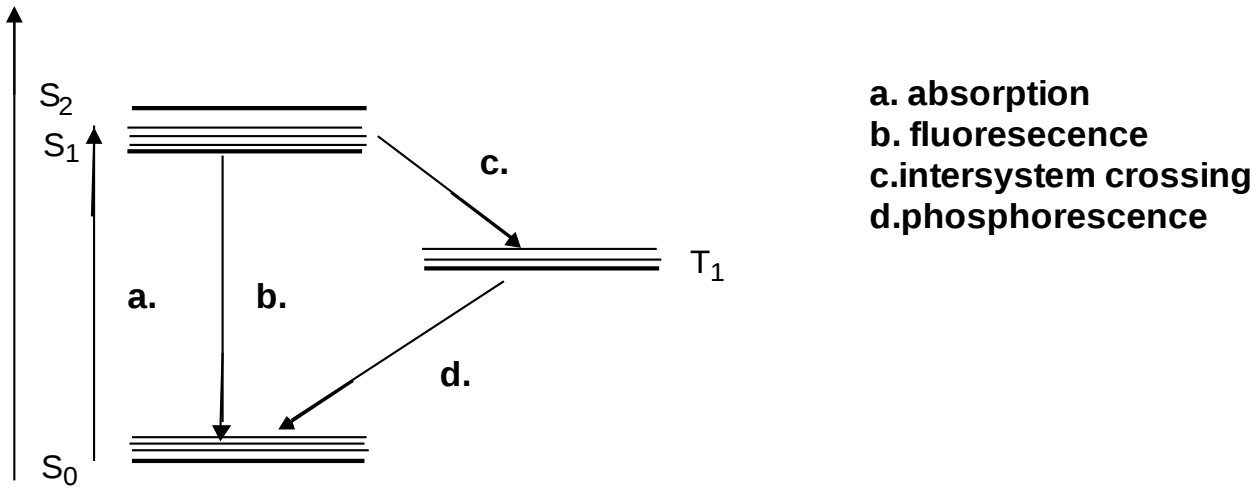

Figure 5

An excited system S_1 or T_1 tends to lose the energy (to relax) by colliding with the solvent molecules and decay to the lowest vibrational state of this excited state. The emission of photon comes from this level and represents an example of the Kasha rule for which the luminescence on the polyatomic molecules take place fundamentally from the the lowest level of the excited state. The fluorescence energy is lower than the absorption energy since the molecule lose some of the energy before it emits the photon, and the difference on this the energy is known as Stokes shift. The triplet sate is populated by indirect ways by the singlet states via intersystem spin-crossing, S_1 to T_1^{v} (vibrational excited levels

of the triplet state) and after to T_1. The mean lifetime of T_1 state is on the order of 10^{-3} s greater than that of the singlet (< μs). The energy of T_1 is lower than that of S_1 (Hund's law) so the transition, despite spin forbidden, it is energetically favourable and for some molecule it takes place (ex., benzophenone). In other systems the transition is promoted by the presence of atoms of high atomic number, *Heavy Atom Effect*.

On the mechanism of energy transfer occurs the deactivation (quenching) of the excited state by the presence of a molecule on its ground state. This mechanism of intermolecular transfer energy is the base of the process photodynamic was described by the first time by two Russian scientists (Terenin and Ermolaev).

On their experiment, a solution of acetophenone (PhCOMe) in ether-ethanol (at 90 K) was irradiated at 366 nm and the phosphorescence was registered at 388 nm. On the presence of naphthalene, the emission disappeared and appeared an emission at 470 nm corresponding to the naphthalene phosphorescence (figure 6). Given that naphthalene does not absorb at this wavelength the most plausible interpretation was that naphthalene was excited to triplet state by the energy of acetophenone. On the role process acetophenone represents the donor and naphthalene the acceptor, the quencher of acetophenone phosphorescence. The energy of the triplet sate of the donor should be grater than the the energy of triplet state of the acceptor.

A last and important concept is the quantum yield of a photochemical process, defined as the ratio of excited molecules that goes a given process. For example, Φ_F and Φ_P are the fluorescence and phosphorescence quantum yields, Φ_{ISC} the intersystem crossing one, Φ_T and Φ_S the triplet and singlet formation quantum yields. An actinometer is used to determine the number of photon incident that represents the the number of molecules getting excited. Knowing all the possible processes the sum of all quantum yields should be one.

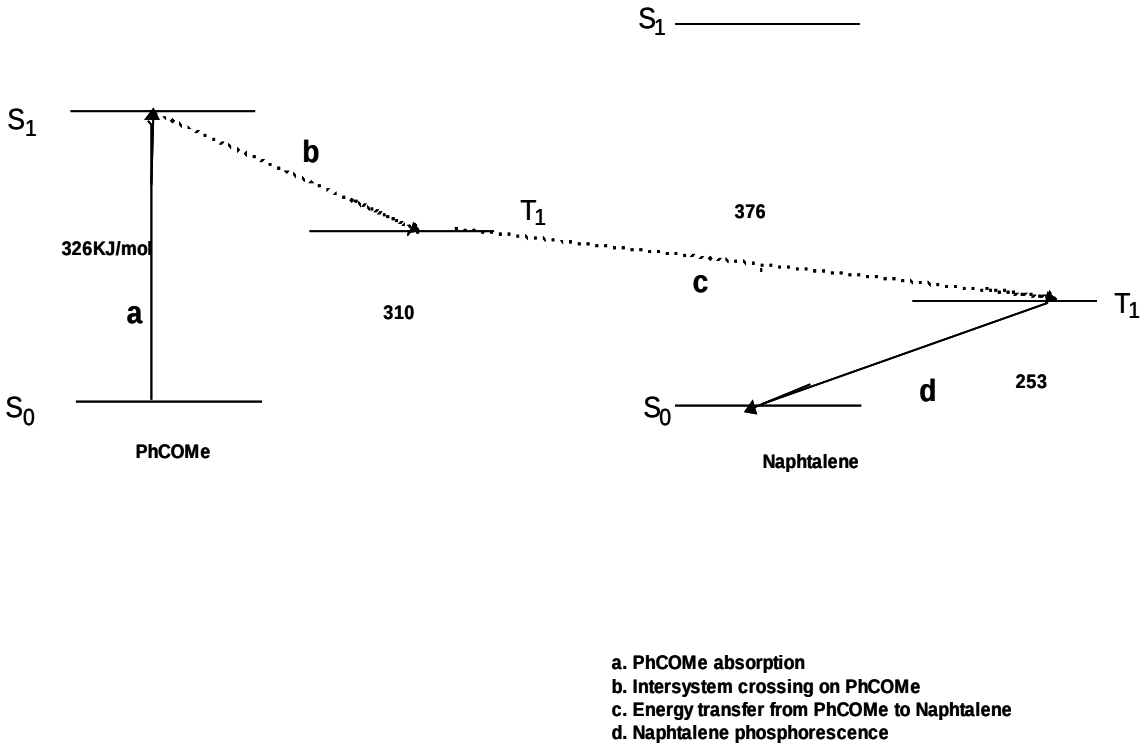

Figure 6

Singlet molecular oxygen on Photodynamic Therapy

The O_2 ground state configuration is $KK(\sigma_g 2s)^2\ (\sigma^*_u 2s)^2\ (\sigma_g 2p\ )^2\ (\pi_u 2p)^4\ (\pi^*_g 2p)^2$. The HOMO[1] orbital $\pi^*_g 2p$ is doubly degenerate. On the ground state each one of the two $\pi^*_g 2p$ orbitals is occupied by one electron giving rise to triplet state $^3\Sigma_g^-$, explaining the paramagnetic property of dioxygen. With the same occupation but now the electrons having anti parallel spin originates a singlet state $^1\Sigma_g^+$ while with the two electrons at the same HOMO orbital gives rises to an another singlet state $^1\Delta_g$. The energies of the $^1\Delta_g$ and $^3\Sigma_g^-$ lye on 0.98 eV (22.5 kcal mol^{-1}) and 1.37 eV (31.5 kcal mol^{-1}) respectively (figure 7).

As we will see the specie $^1\Delta_g$ is the key molecule on the process of PDT.

The state $^1\Delta_g$ has a long life meantime of 45 mn since the decay to the ground state is spin forbidden while $^1\Sigma_g^+$ has a short life meantime of 7-12 s since the transition to the ground state is spin allowed.

In solution the mean lifetime reduces to 10^{-6}-10^{-3} s for $^1\Delta_g$ and 10^{-11}-10^{-9} s for $^3\Sigma_g^-$. The transition $^1\Delta_g \rightarrow {}^3\Sigma_g^-$ is observed experimentally at 1268.7 nm on absorption and emission despite it is forbidden by spin

1 Highest Occupied Molecular Orbital

and symmetry.

Singlet oxygen can be generated by chemical or physical methods. Chemically it is formed by the reaction of hydrogen peroxide with sodium hypochlorite (figure 8).

Physically, singlet oxygen is formed by direct excitation, microwave discharge or by photo sensitization. The last way is the most used in laboratory and on the PDT.

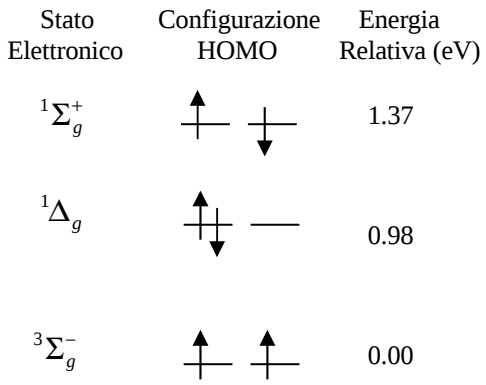

Figura 7

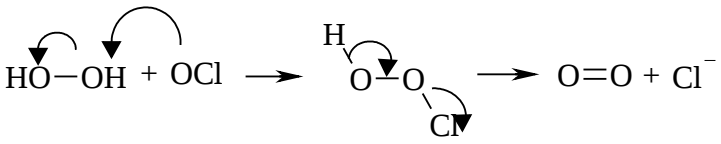

Figura 8

Molecular mechanisms of PDT

The first step on the mechanisms of PDT involves the excitation of the ground state S_0 to the first excited singlet state S_1. It may then, through intersystem crossing, come to reside in the relatively long-lived first excited triplet state T_1

$$Ps(S_0) + h\nu \rightarrow Ps(S_1) \qquad \text{(Excitation)}$$

$$Ps(S_1) \rightarrow Ps(T_1) \qquad \text{(Intersystem crossing)}$$

Oxygen-dependent type I

In this mechanism the triplet state is reduced by an electron donor (e.g. one of the DNA bases), followed by electron transfer from the reduced photosensitiser to molecular oxygen resulting in formation of reactive superoxide anion radicals

$$Ps(T_1) + D \rightarrow Ps^{\bullet -} + D^{\bullet +} \qquad \text{(Reduction)}$$

$$Ps^{\bullet -} + {}^3O_2 \rightarrow O_2^{\bullet -} + Ps \qquad \text{(Electron transfer, ET)}$$

The eventual cytotoxic action is not due to the superoxide anion $O_2^{\bullet -}$ which is not so reactive. However its protonated form brings to hydrogen peroxide which, on the absence of enough amount of its degrading enzyme catalase and on the presence metallic ions, generates irreversible changes on macromolecules on the cell.

oxygen-dependent type II

In oxygen-dependent type II reactions (electron-exchange type mechanism) the excitation energy of the first excited triplet state of the drug is transferred to molecular oxygen.

$$Ps(T_1) + {}^3O_2({}^3\Sigma) \rightarrow Ps(S_0) + {}^1O_2({}^1\Delta)$$

The excited singlet molecular oxygen in turn reacts rapidly and essentially without discrimination with a wide variety of biomaterials A, and thus cause severe damage.

$$\mathbf{{}^1O_2 + A \rightarrow AO_2}$$

This model was proposed for the first time by Kautsky at 1937. Schönberg (1935) had proposed another mechanism without the generation of singlet oxygen. For Schönberg, the excited drug (T_1) would react with oxygen to form an adduct which one would react with the biomaterial A to form AO_2 and releasing the drug. Kautsky on 1933 published a work with the demonstration of singlet oxygen generation. The experiment supposed the existence of $^1O_2$ in gas phase where the adduct of Schönberg would have a low vapour tension. On the procedure they fixed two micelles from silica gel particles. On the first micelle came absorbed acriflavine (the photosensitizer) and on the other absorbed leuco-malachite, an uncoloured molecule representing the biomaterial A. After irradiation at adequate oxygen pressure the leuco-malachite passes from uncoloured to green. Kautsky proposed the formation of an activated form of oxygen which after diffusion has oxidized the uncoloured molecule. Experiments conducted 30 years after by Foote and Wexler, and Corey and Taylor confirmed the presence and rule of singlet oxygen.

Direct electron transfer

One could also imagine a direct oxidation of the drug by oxygen

$$Ps\ (S_0 / T_1) + {}^3O_2 \rightarrow Ps^{\bullet -} + O_2^{\bullet -}$$

Autoionization

The drug in its T_1 state is reduced by another molecule of the drug in its T_1 or S_0 state, thereby forming a radical anion–radical cation couple

$$Ps(T_1) + Ps(T_1) \rightarrow Ps^{\bullet -} + Ps^{\bullet +}$$

$$Ps(T_1) + Ps(S_0) \rightarrow Ps^{\bullet -} + Ps^{\bullet +}$$

On type II mechanism the triplet state of the drug transfers its energy to oxygen ground state generating

singlet oxygen. To this transference to be efficient the energy of the triplet state of the drug should be greater then 95 kJ/mol (0.98 eV) of the singlet oxygen. Chemically, the efficacy of a drug on the PDT is measured by the oxygen singlet quantum yield Φ_Δ.

For example, for 8-MOP and acridine the Φ_Δ is respectively 0.83 (in benzene) e 0.009 (deuterated water) while for hematoporphyryn it is 0.52 (in methanol). The $^1O_2$ Φ_Δ is a product of two factors

$$\Phi_\Delta = \Phi_T.\Phi_{en}$$

where Φ_T is the triplet quantum yield and Φ_{en} is the energy transfer quantum yield which can be calculated by the kinetic constants

$$\Phi_\Delta = \Phi_T \Phi_{en} = \Phi_T \frac{k_{en}[O_2]}{k_r + k_{nr} + k_q[O_2]}$$

k_{en} is the kinetic constant for energy transfer, k_r and k_{nr} the kinetic constant for radiative and non radiative deactivation of the triplet state and k_q the sum of the kinetic constants relative to the deactivation of the triplet state by oxygen (quenching).

The distinction between type I and II mechanisms can be done by some basic experiments. For example, the revelation of $^1O_2$ by luminescence, the quenching of formed $^1O_2$ with 9,10-diphenylanthracene with the formation of endoperoxides or the reaction with cholesterol giving 5α-hidroperoxide are some ways to confirm the type II mechanism. Also when the same results, namely tissue destruction, are obtained without the drug but on the presence of $^1O_2$ generated by reaction between NaOCl/H2O2 or by microwave discharging, type II mechanism is confirmed.

On the following we discuss some experimental methods to reveal singlet oxygen and so the type II mechanism:

Luminescence

the appearing of luminescence on the micelle reaction is due two processes. One is at 1270 nm and correspond to singlet oxygen radiative deexcitation

$$^1O_2 \rightarrow {}^3O_2 + h\nu \qquad (1270\ nm)$$

This emission is not so intense since it is spin forbidden ($T_1 \rightarrow S_0$) but it fails at region of the spectra free of biomaterial emission, so it is a direct method to reveal $^1O_2$.

The second is at higher energy and results from the interaction of two excited oxygen molecules

$$2\,^1O_2 \rightarrow 2\,{}^3O_2 + h\nu\ (634,\ 704\ nm)$$

chemical reaction

the presence of molecules that react with $^1O_2$ decreases the rate of tissue destruction. Examples of these reactants are 1,3-diphenylisobenzofuran and 9,10-diphenylanthracene. On the last case the the molecule consumption can be monitored by spectroscopic methods since this molecule have a chromophore group.

$^1O_2$ *quenching*

Molecules like β-carotene (figure 9) deactivate $^1O_2$ by an energy transfer mechanism (figure 10)

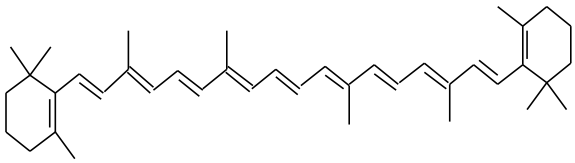

Figure 9

since it has a triplet energy lower than 94 KJ/mol.

The electromagnetic radiation on PDT: source and wavelength

The optimal properties of the light to be used on PDT will be discussed on this section. We discuss the principal sources of light to be used on PDT and on the successive paragraph we report on the question light penetration on the tissue.

The source of light

The incandescent lamp

This kind of lamp are the first source of light used on PDT. They are constituted by a metallic filament (eg tungsten) protected by a glass bulb which is heated by an electric current. The incandescent lamp is economic and was used for the treatment of Basal-Cell Carcinoma with δ-aminolevulinic acid as PDT drug.

Arc Lamp

The mercury arc lamp is amply used in organic photochemistry and also in photomedicine. There are three kinds depending on the pressure the mercury is: low (10^{-3} mm of Hg), medium (1 atm) and high (100 atm). The low pressure lamp works at normal temperature and has just one emission line at 253.7 nm (UV-C, figure 3) and for this reason is used also as Germicidal lamp. The medium pressure lamp has several lines of emission but the principal ones fail on 366 at 546 nm. If the radiation is filtered with Wood's glass only the UV (366 nm) remains, and it is only used for the fluorescence of porphyrin or others molecules. The lamp at high pressure forms a continuum spectra of emission, however requires a refreshing system and have short duration. The lamps that use xenon or xenon-mercury are intense, more economic, work at 20 atm and don't require refreshment. For both the sources, incandescent and arc lamps, is possible

Light-emitting diode

The Light-emitting diodes (LEDs) are semi conductors light sources (III and IV groups of the periodic table). The emission of light is not coherent, the power is low and for this reason does not produce too much heat. The wavelength is modulated according to the semi conductor used and also the devices are small and adaptable to the specific zone the tumor is.

Lasers

the laser is the most advanced light source. It is based on a process of stimulated emission by an excited state from a sample with inverted population, meaning that the excited state is significantly more

populated then in an equilibrium situation. The emitted radiation is intense, coherent and monochromatic however on laser the devices are more expensive then on the other sources. The most common lasers are in solid state, with argon and an organic colorant which allows the modulation of light frequency. For example, Rodamina-6G has fluorescence on the range 570-620 nm, and the frequency of the laser can modulated in function of the PDT agent.

Photosensitizers on PDT

On the precedent paragraphs we mentioned some requisites a molecule should contains to be a an efficient drug on PDT. Firstly, we show that on the type II mechanism the triplet energy of the drug should be greater than the 95 KJ/mol of singlet oxygen. Concerning the radiation to be used we noticed that is should be on therapeutic window of 650-850 nm. Because of this, the drug should have the transition $S_0 \rightarrow S_1$ on this range. For chemical point of view these two conditions govern the research for new drugs. Also, there is another conditions, like clinical related to permeability of drug or the collateral effects on the body.

On the following paragraphs we introduce the photosensitizers of the first generation, after the ones of the second generation developed to correct some inconvenient properties. At the end to review the actual state on PDT research.

First generation Photosensitizers

The derivatives of hematoporphyrin (figure 10) and commercial variants (hotofrin, Photosan, Photogem e Photocarcinorin) historically they belong to the first generation of photosensitizers developed to be applied on PDT. We already mentioned the history of the HPD origin. Now, we focus on the the synthesis and properties of the commercial variant Photofrin.

This derivative is synthesized by making react the hematoporphyrin in a micelle of sulfuric and acetic acids, forming hematoporphyrin-IX di and mono acetate (Fase I HpD). The alkaline hydrolysis gives a micelle containing monomer, dimer and oligomer of HpD. The capacity od HpD as drug is due to the oligomer component. The micelle with the dimer and oligomer can be separated by HPLC and the obtained fraction enriched on the oligomer is named D Fraction. From this fraction is obtained the commercial forms. The ratio between the monomer, dimer and oligomer is 22:23:55 on HpD while for

Photofrin it is 14:19:67 and in this case the larger oligomer observed contains nine porphyrin like units.

Although Photofrin does not exhibit systematic toxicity or mutagenic effects and also have been used for several tumor kinds, it has some inconveniences.

In particular, the oligomeric form tends to form agregates that does not give the same singlet oxygen quantum yield (Φ_{Δ}=0.20 against Φ_{Δ}=0.65 for the monomeric form of hematoporphyrin).

However the principal cause to keep Photofrin very far from being and ideal drug on PDT is its absorption spectra, moreover very similar to the HpD spectra. The HpD spectra contains a very intense band at 400 nm (Soret band) and others bands with decreasing intensity at 500, 540, 570 and 630 nm (Q band). The band at 630 nm is the one used on PDT since is one with larger penetration. However this band is very weak (ε = 3000 M^{-1} cm^{-1}) requiring a high administration dose on patient what will increase the risk of collateral effects.

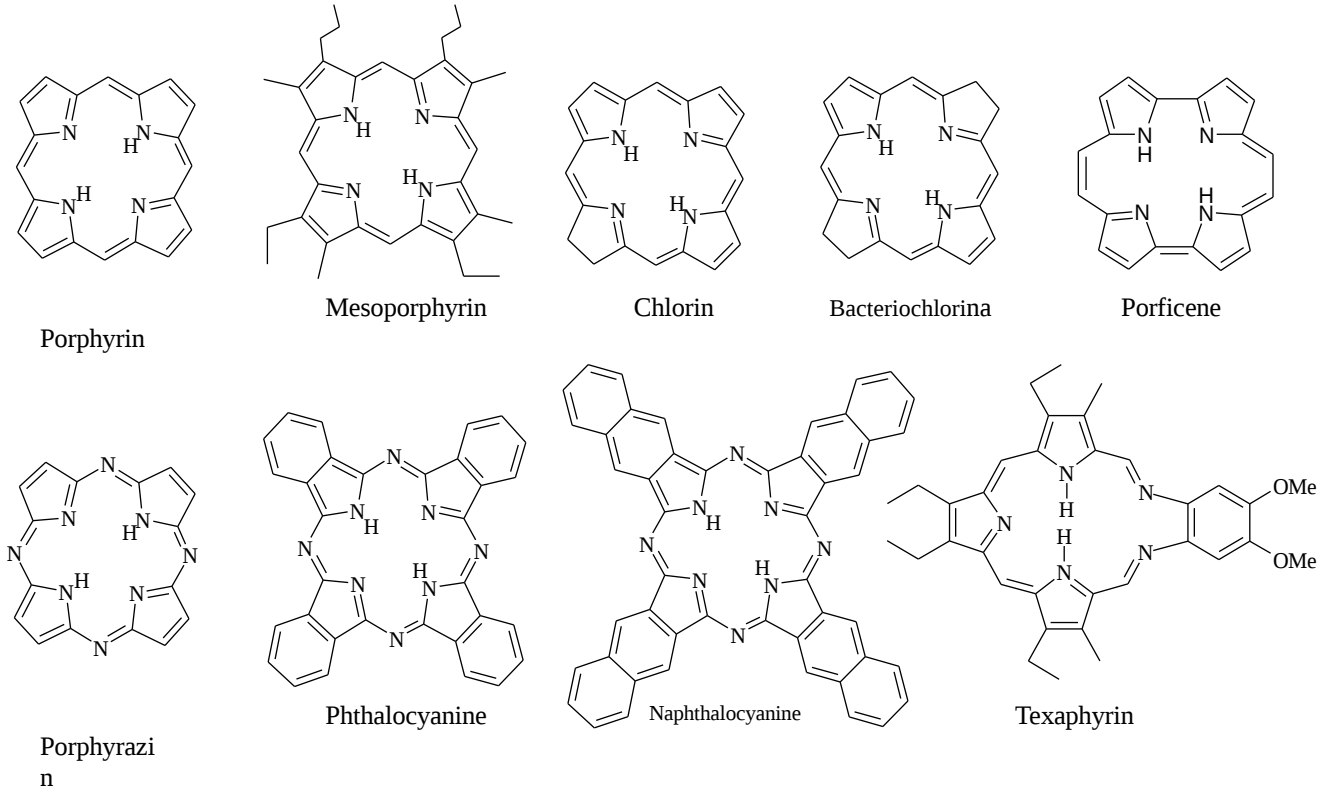

Figure 10

Second Generation Photosensitizers

The advantages and disadvantages of HPD and its derivatives experimented during clinic application have allowed the definition of the most important criteria on the synthesis the new drugs that are labeled by Second Generation Photosensitizers. To improve the efficacy of the drugs on PDT, the scientists have the following criteria on their procedures: a) toxicity on the absence of the drug or dark toxicity, b) synthesis and composition, c) the properties on solution, d) the photophysical properties, e) Absorption on the red part of the spectra.

toxicity on the absence of the drug or dark toxicity

The drug should have low dark toxicity to permit a good control of tumor in function of the drug dose and radiation quantity. Some tetrapyrrols derivatives (eg. porphyrin) satisfy other criteria but are not ideal since they have a high toxicity.

synthesis and composition

As we saw the the HpD derivatives is constituted by a micelle of composts (monomers, dimers and oligomers) whose relative quantities depend on the syntheses conditions becoming difficult to establish a correlation between the drug dosage and the therapeutic effect. Also the HpD (figure 2) has two stereoisomers becoming difficult to know the reactive toxicity of each isomer. For this, it is important to use a simple substance with defined compositions to establish good dose/effect correlation. On PDT exists other variable to be considerated like the time interval between the administration of the drug and irradiation, the wavelength od the radiation, its total energy and the radiation flux. Regarding the synthesis, it should be simple and produce a good yield ad the final drug should be stable kinetic and thermodynamically.

properties on solution

An ideal drug on PDT should localize preferentially on the tumor zone and, at the same time, be easily removed after the theraphy. The majority of the drugs are constituted by a porphyrin macro cycle (eg. Porphyrin, chlorine, figure 11) or porphyrin like (eg. Ftalocyanine, texaphyrin, figure 10) that has hydrophobic character while the cellular environment, where the molecule may act, is aqueous.
For this reason, in these molecules are incorporated on the synthesis process polar groups like sulfonic,

carboxylic, hydroxil or quaternary ammonium. These functional groups confer to the drug an amphiphilic (hydrophlic+hydrophobic) character.
To solve the problem of solubility another possibility is the transportation of the PDT agent by micelles or related structures.

To increase the drug stability on solution and avoiding this way the precipitation that makes the dug inactive specific molecules are incorporated on the drug. An example, is the use of synthetic molecules (neutral or ionic) similar to the detergents like Tween 80 or Cremophor EL. These molecules contain polar groups at one side and apolar groups at other side and can act as a emulsifier for the drugs in aqueous environment.

the photophysical properties

A drug for PDT should have a triplet energy larger then 94 KJ/mol, a good triplet quantum yield Φ_T, a good mean lifetime, τ_T, in order to react with the triplet oxygen to form singlet oxygen. Being singlet oxygen the principal actor on PDT, a parameter that measure better the efficacy of a drug is the singlet oxygen quantum yield Φ_Δ. On table 2 we show some important photophysical for several drugs.

Table2 . Fluorescence Φ_F, triplet Φ_T and singlet oxygen Φ_Δ quantum yields, triplet mean lifetime τ_T for several tetrapyrroles macro cycles

Classe	Complex	Solvente	Φ_F	τ_T (μs)	Φ_T	Φ_Δ	
Porphyrin	Tetraphenylporfyrin	toluene	0.10	>10	0.73	0.67	Ref.1
	Zn-Tetraphenylporphyrin	toluene	0.333	>10	0.86	0.68	Ref.1
	Cu- Tetrapheniphorpyrin	toluene	0	0.00178	0.88	0.03	Ref1
Chlorine	octaetilpurpurina	benzene			0.82	0.67	Ref2
	Zn-etiopurpurina	benzene			0.83	0.57	Ref.2
Bacterioclorine	Bacteriochlorophyll a	benzene			0.32	0.32	Ref.2
	Bacteriopheophytin a	benzene			0.73	0.46	Ref2
Ftalocianine	phthlocyanine	$C_{10}H_7Cl$	0.7	140	0.14	0.16	Ref3,4,5
	Al(III)-phthlocyanine	$C_{10}H_7Cl$	0.58	500	0.4	/	Ref4,6
		dmso	/	/	/	0.29	Ref
	Zn-phthlocyanine	$C_{10}H_7Cl$	0.3	125	0.65		Ref3 6
		dmso	/	/		0.4	Ref
	Si-naphthalocyanine	benzene			0.39	0.35	Ref2
Porficene	Porficene	toluene	/	/	0.42	0.30	Ref2
Texaphyrin	Lu(III)-texafirina					0.31	Ref. 7

Absorption on the red part of the spectra

We discussed on paragraph 1.3 that the λ_{max} of the drug should be on the red part of the spectra (600-850 nm) in order to better penetrate the the biological tissue. On table 3 are reported values of λ_{max} for porphyrin and porphyrin like systems. We notice the difference on λ_{max} between porphyrin (600-640 nm) and Naphthalocyanine (780 nm), also the difference on ε (1:100).

The radiation should be on the therapeutic window, on the range 650-800 nm. Molecules absorbing on larger wavelength (infrared) have their use limited for several factors. First, on the infrared region the water molecule of tissue absorbs the radiation, reducing the light that reach the tumor, second to the molecule to absorbs at infrared it needs to have a low HOMO-LUMO gap what implicates that the molecule is more easily oxidized resulting in photobleaching, the phenomenon of absorption (or fluorescence) property loss by chemical modification of the chromophore. A third reason occurs when type II mechanism is in action. The energy of the triplet should be greater than 94 kJ mol^{-1} (1270 nm) of the singlet oxygen. The singlet state S_1 that generates the triplet T_1 lower in energy by the Hund should itself be higher in energy than 94 kJ mol^{-1}.

Table 3. Porphrin like compounds: maximum absorption wavelength and extinction coefficient

	λ_{max} (nm)	ε ($M^{-1}cm^{-1}$)
Pophyrin	620-640	3500
Chlorine	680	40000
Bacteriochlorine	780	150000
Porphyrin Meso- substituted	650	18000
Phthalocyanine	700	200000
Naphthalocyanine	780	350000
Porficeni	610-650	50000
Texaphyrin	732	42000

In conclusion the criteria for the synthesis of PDT drug of the second generation should follow a balance between photophysical and and solubility criteria.

Actual state on PDT research

Nowadays at the same time scientists look for new second generation drugs is being developed methods for the drug delivery. One of this method is Antibody (Ab)-based drug delivery. This strategy consists of linking the drug with monoclonal antibodies (MoAb) against specific antigens of malignant cells. This method explores the known fact that there are characteristic differences between tumour and normal cells, e.g., higher expression of specific antigens and onco proteins by cancer cells. These new drugs are called third generation photo sensitizers.

Bibliography

(1) Bonnett, R. *Chemical Aspects of Photodynamic Therapy* Gordon and Breach Science Publishers: Amsterdam, **2000**.

(2) Bonnett, R *Rev. Contemp. Pharmacother*, **1999**, *10*, 1-19.

(3) Regan, J. D. and Parrish J.A. *The Science of Photomedicine*, Plenum, New York and London, **1982**

(4) Finsen, N. R. *Phototherapy*, Arnold, London, **1901**.

(5) Jori, G. and Perria C. (Eds) *Photodiagnostic and Phototherapeutic Techniques in Medicine*, Documento Editoriale, Milan, **1995**.

(6) Bicknell, F. and Prescott *The Vitamins in Medicine*,, Heinemann, London, **1942**, 442-503.

(7) Parrish, J. A., Fitzpatrick, T. B., Tanenbaum, L., Pathak, M. A. *N. Engl. J. Med.*, **1974**, *291*, 1207-1222.

(8) Cremer, R. J.; Perryman, P. W.; Richards, D. H. *Lancet*, **1958**, 1094-1097.

(9) Bock, G. and Harnett, S. (Eds) *Photosensitising Compounds: Their Chemistry, Biology and Clinical Use*, Ciba Foundation Symposium 146, Wiley, London, **1989**.

Harris, D. C. and Bertolucci M. D. *Symmetry and Spectroscopy*, Dover Publications, inc.,New York, **1989**

Atkins, P. W. *Molecular Quantum Mechanics*, Oxford University Press, Oxford, **1983**

Turro, N. J. *Modern Molecular Photochemistry*, University Science Books, **1991.**

THEORETICAL METHODS

Quantum mechanical foundations

At the end of the 19 th century the unsuccessful application of classic physics laws to microscopic systems, atoms and molecules, showed the limits of classical mechanics and have brought to the emergence quantum mechanics. The quantum mechanics study of the stationary properties of microscopic systems and their evolution on time have the basis on the equation proposed on 1926 by the Austrian physicist Erwin Schrödinger from who it takes the name.
The Schrödinger equation has analytical solution only for hydrogen like systems (one electron and one nuclei), for others systems numerical solution is the alternative however the it become more difficult with increase size of the system.
On Quantum Mechanics, due to the Heisenberg principle of Uncertainty the state of a system cannot be descripted by its position and velocity. However all the information we can have about the molecular system is contained in a wave function Ψ(r,t) depending on the time t and on the positions of all particles r. The analysis in terms of the wave function is very difficult for a large system since the wave function depend on the 3N spacial coordinates plus N spin coordinates (4N).
For these inconveniences were developed a simpler theory named Density Funtional Theory DFT where the electron density take the place of the wavefunction. The density depends only on a one parameter, it associates to a point in space to its electron density, what constitutes an advantage over the wavefunctions theory. The accurate mathematical treatment by DFT results of gradual theoretical contributions from the first tentative at the ends of the sixties with the introduction of the Thomas-Fermi model on evaluating the energy of a multielectronic systems without using the wavefunction. By these model the average potential of a homogeneous electron gas is expressed by the electron density.
At the begins the density approach was more a tentative to express any contribution of the energy as dependency on the density. With the publications of two mathematical theorems the Thomas-Fermi model is seen as an approximation, despite inaccurate, of a general theory named Density Functional Theory.
Since the majority of results obtained by DFT is confirmed by the traditional ab initio methods, on the next paragraphs we show the basic differences between these two approaches.

The Hartree Fock (HF) method

The compact formulation of time independent and non relativistic Schrödinger equation is

$$\mathrm{H}\left|\Phi\right\rangle = E\left|\Phi\right\rangle \tag{1}$$

on the case of a molecular system with N nuclei and M electrons the Hamiltonian operator is

$$\hat{\mathrm{H}} = -\sum_{i=1}^{N}\frac{1}{2}\nabla_i^2 - \sum_{A=1}^{M}\frac{1}{2M_A}\nabla_A^2 - \sum_{i=1}^{N}\sum_{A=1}^{M}\frac{Z_A}{r_{iA}} + \sum_{i=1,j>i}^{N}\frac{1}{r_{ij}} + \sum_{A=1,B>A}^{M}\frac{Z_A Z_B}{R_{AB}} \tag{2}$$

The first and second terms are the nuclear and electronic kinetic contributions to H, while the third, fourth and fifth are electrostatic potential energy referring to: nucleus-electron attraction, electron-electron repulsion and nucleus-electron repulsion. M_A and Z_A are the mass and charge of nucleus A,

r_{iA} the distance between electron i and nucleus A, r_{ij} the distance between electrons i and j and R_{AB} the distance between nuclei A and B.

Thanks to a fundamental result named Born-Oppenheimer Approximation, by the difference in mass between the nucleus and the electron, it is possible to separate the molecular problem in two problems, the nuclear problem and electronic problem, and simplify the equation 2. It becomes possible to solve 2 considering the nuclei fixed, writing an electronic Hamiltonian operator without the nuclear kinetic operator

$$\hat{\mathrm{H}}_{el} = -\sum_{i=1}^{N}\frac{1}{2}\nabla_i^2 - \sum_{i=1}^{N}\sum_{A=1}^{M}\frac{Z_A}{r_{iA}} + \sum_{i=1,\,j>i}^{N}\frac{1}{r_{ij}} \qquad (3)$$

or synthetically

$$\hat{\mathrm{H}}_{el} = \hat{\mathrm{T}} + \hat{\mathrm{U}}_{ee} + \hat{\mathrm{U}}_{ext} \qquad (4)$$

Concerning the electronic wave function associated with $\hat{\mathrm{H}}_{el}$ the first proposal was by Hartree was to consider a a product of monoelectronic wavefunctions (Hartree product). However this product didd not respect the wave functions antissymmetry resulting from the Pauli principle.

The best approximation is an antissymetrized product or a Slater determinant of N spin orbitals $\chi_i(x)$

$$\Psi_{HF}(x_1, x_2, ..., x_N) = \frac{1}{\sqrt{N!}}\begin{vmatrix} \chi_1(x_1) & \cdots & \chi_i(x_1) & \chi_j(x_1) & \cdots & \chi_N(x_1) \\ \chi_1(x_2) & \cdots & \chi_i(x_2) & \chi_j(x_2) & \cdots & \chi_N(x_2) \\ \cdot & & \cdot & \cdot & & \cdot \\ \cdot & & \cdot & \cdot & & \cdot \\ \cdot & & \cdot & \cdot & & \cdot \\ \chi_1(x_N) & \cdots & \chi_i(x_N) & \chi_j(x) & \cdots & \chi_N(x_N) \end{vmatrix} \qquad (5)$$

The factor $1/\sqrt{N!}$ is the normalization factor.

The energy of the state Ψ is given by

$$E[\Psi] = \frac{\langle \Psi | \hat{H}_{el} | \Psi \rangle}{\langle \Psi | \Psi \rangle} \tag{6}$$

which applied to the Slater determinant splits the energy in three terms

$$E_{HF} = \langle \Psi_{HF} | \hat{H}_{el} | \Psi_{HF} \rangle = \sum_{i=1}^{N} h_i + \frac{1}{2} \sum_{i,j=1}^{N} (J_{ij} - K_{ij}) \tag{7}$$

where h_i is the Core Hamiltonian for electron i, that results on the sum of its kinetic energy with the interaction with nuclei, $v(x)$

$$h_i = \int \chi_i^*(x) \left[-\frac{1}{2} \nabla_i^2 + v(x) \right] \chi_i(x) dx \tag{8}$$

J_{ij} is the coulombic repulsion between an electron on the state χ_i and another electron on the state χ_j

$$J_{ij} = \int\int \chi_i^*(x_1) \chi_i(x_1) \frac{1}{r_{12}} \chi_j^*(x_2) \chi_j(x_2) dx_1 dx_2 \tag{9}$$

K_{ij} is the exchange integral, appears as a consequence of the antisymmetric product and has no analogy in classical physics.

$$K_{ij} = \int\int \chi_i^*(x_1) \chi_j(x_1) \frac{1}{r_{12}} \chi_i(x_2) \chi_j^*(x_2) dx_1 dx_2 \tag{10}$$

On HF method each orbital χ_k is a product of a spacial orbital by a spin orbital. The spacial orbital is an expansion on a basis set, being its energy dependent on expansion we use. However there is a result named Variational Principle that permits the determination of the best solution for the ground state energy – the best approximation for the ground state wavefunction gives the minimum energy.

$$E_0 = \min_{\Psi_{HF}} E[\Psi_{HF}] \tag{11}$$

With the normalization conditions

$$\int \chi_i^*(x)\chi_j(x)dx = \delta_{ij} \tag{12}$$

we need to find the wavefunctions that minimizes the energy

$$\delta E[\Phi]_{\Phi=\Psi_0} = 0 \tag{13}$$

The application of variational method to the HF wavefuction brings to the HF equations:

$$\hat{F}|\chi_i(x)\rangle = \sum_{j=1}^{N} \varepsilon_{ij}|\chi_j(x)\rangle \tag{14}$$

$$\hat{F} = -\frac{1}{2}\nabla^2 + v + (\hat{j} - \hat{k}) \tag{15}$$

where ε is a hermitian matrix ($\varepsilon_{ij} = \varepsilon_{ij}^*$) meaning that all of the eingenvalues are real and can be associated with measurable quantities. It is important to know that the Fock operator is a function of the spin-orbitals χ_k through the coulombic $\hat{j}$ and exchange $\hat{k}$ operators:

$$\hat{j}(x_1) f(x_1) = \sum \int \chi_k^*(x_2)\chi_k(x_2)\frac{1}{r_{12}} f(x_1)dx_2 \tag{16}$$

$$\hat{k}(x_1) f(x_1) = \sum \int \chi_k^*(x_2) f(x_2)\frac{1}{r_{12}} \chi_k(x_1)dx_2 \tag{17}$$

For this reason the Hartre Fock equation is solved by an interactive way from an trial set χ_k where the solutions will be used to form a new fock operator in a new cycle. The process continues until there is

no more significant change in important quantities, like the density. At this moment we reach self consistency and the method is known as SCF (Self Consistent Field).

The mathematical solutions of the equation (14) is simplified noticing that any linear combination of the spin-orbital are still solution of the same problem

$$\left|\varphi_{\mu}\right\rangle = \sum_{k} U_{\mu k}\left|\chi_{k}\right\rangle \tag{18}$$

where U is an unitary matrix ($U^{+}U = 1$). The equation (14) becomes

$$\hat{F}\left|\varphi_{\mu}\right\rangle = \sum_{j=1}^{N} \varepsilon_{j\mu}\left|\varphi_{j}\right\rangle \tag{19}$$

where the new matrix ε is obtained from the old one by

$$\varepsilon = U\varepsilon U^{+} \tag{20}$$

by choosing U as a matrix that diagonalizes ε we obtain the canonical form of the HF equation

$$\hat{F}\varphi_{\mu} = \varepsilon_{\mu}\varphi_{\mu} \tag{21}$$

The correlation energy and the CI method

The limit of the Hartree Fock method is to describe the energetic contribution due to the correlation between the electrons with opposite spin named as correlation energy. The use of the mono determinante wavefunction is just a good approximation for the real wavefunction of a multi electronic system since it does not take explicity the the instantaneous interaction between the electrons. Given an electron in a position close to the nucleus at a certain time, by energetic repulsion, is makes is unprovable to find another electron close to this nucleus a the same time.
So, an electron induces an *absence o*f electron density around itself, named as Coulomb hole, showing that the electrons are correlated.
Besides the Coulombic correlation there is the the exchange correlation arising from the antisymmetric nature of the wavefunction that makes impossible to find two electrons with opposite spin at the same position. A Fermi hole is said to exist around an electron.

The only way the Slater determinant considers the correlation energy is by giving zero to the probability the finding two two electrons with opposite spin at the same position.

To take account the electron correlation we can substitute the Slater monodeterminant by a wave function that includes excited electron configurations

$$\Phi_{CI} = \left|\Phi\right\rangle = C_0\left|\Psi_0\right\rangle + \sum_{ir} C_i^r \left|\Psi_i^r\right\rangle + \sum_{\substack{i<j \\ r<s}} C_{ij}^{rs} \left|\Psi_{ij}^{rs}\right\rangle + ... \qquad (21)$$

The maximum number of Slater determinant that can be constructed depends on the number electron (N) and on the number of spin-orbitals (2K), is given by $\binom{2K}{N}$. However, the number and kind of excitations used is truncated in function of the particular system on study and on the computational cost.

The energy obtained by the application of the variational method is the the exact non-relativistic energy E and the difference between it and the HF energy E_{HF} obtained in the limit the basis set approaches completeness is the correlation energy

$$E_{corr}^{HF} = E - E_{HF} \qquad (22)$$

The DFT method

While the Hartree Fock method is not so accurate because it lacks the correlation between the electrons the CI methods, being more general then the HF method, it is limited by the high computational cost. The theory of density functional permits to treat large systems contemplating the electron correlation with a computational cost lower than CI method, actually comparable with the HF method cost. The focus of DFT is on the electron density, the number electron on a spacial point $r_{1.}$ This quantity can be determinated experimentally and theoretically is calculated through the wave function by

$$\rho(r_1) = N\int...\int\left|\Psi(x_1, x_2, ..., x_N\right|^2 d\sigma_1 dx_2 ... dx_N \qquad (23)$$

Integrating the density on all the space we obtain the total electron number

$$\int \rho(r) dr = N \tag{24}$$

Being that the density is a function of three spacial coordinates ($r=x,y,z$) the DFT method has several advantages that will be discussed on successive paragraphs.

The Hohenberg e Kohn Theorems

The energy of a ground state molecular system is calculated by minimizing the Hamiltonian expectation value of electronic Hamiltonian

$$\hat{H} = \hat{T} + \hat{V}_{ee} + \hat{V}_{est} \tag{25}$$

where $\hat{V}_{ext}$ is the external potential expressed as

$$\hat{V}_{est} = \sum_{i=1}^{N} v(r_i) \tag{26}$$

V_{ee} is specified by the number of electrons N, so the Hamiltonian H comes completely specified by the electron number N and the external potential $v(r)$ for the ground state of a non degenerate system. On the absence of a external field the external potential is the interaction with the nuclei.

The first Hohenberg and Kohn theorem

This theorem states that the density determines univocally the external potential and the electron number, and consequently the Hamiltonian, the energy and the wavefunction of the system.
Any observable associated with an operator O is a functional of the density, including the energy. The kinetic and eletron-electron repulsion part of the total energy are equivalent for all multi electronic system since they don't depend on the particular system depend on external potential. Because of this these two parts are grouped in just one quantity $F[\rho]$, a universal functional

$$F[\rho] = T[\rho] + V_{ee}[\rho] \tag{27}$$

the energy comes given by

$$E[\rho] = T[\rho] + J[\rho] + \tilde{E}_{xc}[\rho] + V_{ext}[\rho] \tag{28}$$

The electron-electron repulsion is separated in two terms, J[ρ], the classical repulsion between the electron given by

$$J[\rho] = \frac{1}{2}\int\int r_{12}^{-1}\rho(r_1)\rho(r_2)dr_1dr_2 \tag{29}$$

and the term $\tilde{E}_{xc}[\rho]$ that makes the quantum correction to J[ρ]. $\hat{V}_{ext}$ represents the average electron-nuclei interaction

$$V_{ext} = \int \rho(r)v(r)dr \tag{30}$$

In a more compact way the energy is given by

$$E[\rho] = F[\rho] + \int \rho(r)v(r)dr \tag{31}$$

The exact knowing of the universal functional $F[\rho]$ permits to calculate correctly the energy of the ground state. However the impossibility of knowing $\tilde{E}_{xc}[\rho]$ and J[ρ] is the principal limitation of DFT theory.

The second Hohenberg and Kohn theorem

This theorems represents the variational method and states that the true density of the a system minimizes its energy. Being $\tilde{\rho}(r)$ a density corresponding to a given external potential $v(r)$ and E_0 the true energy**,** we have that

$$E_0 \leq E_v[\hat{\rho}] \tag{32}$$

Assuming $E_v[\hat{\rho}]$ differentiable the problem of finding the true density consists in finding the stationary point of $E_v[\hat{\rho}]$ with the constrain that the density integrates to the number of electrons

$$\delta\left\{E_v[\rho] - \mu\left[\int \rho(r)dr - N\right]\right\} = 0 \tag{33}$$

from which comes the Euler-Lagrange equation

$$\mu = \frac{\delta E_v}{\delta \rho(r)} = v(r) + \frac{\delta F[\rho]}{\delta \rho(r)} \tag{34}$$

where μ represents the chemical potential.

The Kohn-Sham equations

The first contribute to the determination of kinetic energy functional was done by Kohn and Sham on 1965. They considered a fictitious system constituted by N non-interacting electrons. The kinetic energy and the density of the ground state are known for this ideal system and come expressed as a function of the mono electronic orbitals φ_i

$$T_s[\rho] = \sum_{i=1}^{occ} \langle \varphi_i | -\frac{1}{2}\nabla_i^2 | \varphi_i \rangle \tag{35}$$

$$\rho(r) = \sum_{i=1}^{occ} \sum_{s} |\varphi_i(r,s)|^2 \tag{36}$$

and the Hamiltonian is a sum of monoelectronic orbitals

$$\hat{H}_s = \sum_{i=1}^{N} \left(-\frac{1}{2}\nabla_i^2 + v_s(r_i) \right) \tag{37}$$

The point of the Kohn and Sham approach is to an external potential v_s in a such a way that the density

of the non-interacting system coincides with the density of the real system of interacting electrons.

The real kinetic energy can be written as a sum of two terms

$$T[\rho] = T_s[\rho] + T_c[\rho] \tag{38}$$

where $T_s[\rho]$ is the kinetic energy of the non interacting system and $T_c[\rho]$ takes account of residual part of the kinetic energy due to electronic correlation. In consequence the universal functions can be rewritten as

$$F[\rho] = T_s[\rho] + J[\rho] + E_{xc}[\rho] \tag{39}$$

where the new term $E_{xc}[\rho]$ is the exchange correlation functional and contains also the correlation part of the kinetic energy.

$$E_{xc}[\rho] = T_c[\rho] + \tilde{E}_{xc}[\rho] \tag{40}$$

Using the equations (1.4.17) and (1.4.18) the Euler-Lagrange equation for the real system is

$$\mu = v_{eff}(r) + \frac{\delta T_s[\rho]}{\delta \rho(r)} \tag{41}$$

where $v_{eff}(r)$ is a local monoelectronic potential known as Kohn-Sham effective potential

$$v_{eff}(r) = v(r) + \int \frac{\rho(r')}{|r - r'|} dr' + v_{xc}(r) \tag{42}$$

that includes the exchange and correlation potential $v_{xc}(r)$, a monoelectronic potential

$$v_{xc}(r) = \frac{\delta E_{xc}[\rho]}{\delta \rho(r)} \tag{43}$$

Accepting that the true density is the same of the fictitious system and proceeding with the variational method applied on the space of the orbitals with normalization condition

$$\int \varphi_i^*(x)\varphi_j(x)dx = \delta_{ij} \tag{44}$$

we obtain the Kohn Sham equations

$$\left[-\frac{1}{2}\nabla^2 + v_{eff}(r)\right]\varphi_j = \varepsilon_j\varphi_j \tag{45}$$

The potential we are looking is obtained $v_s = v_{eff}(r)$. Regarding this equation we see that the orbitals appear inn both side. On the left side they are needed to construct the density and then $v_{eff}(r)$ and on the right side they are the solutions we are looking for. Because of this we need a self consistent method we need to use a self consistent method where we part from a tentative density, we calculate the new orbitals as solution, with this new solutions we construct a new density in a new cycle. The process continues until we obtain self consistence.

The difference between the Hartree-Fock and the Kohn-Sham equations resides substantially on the interpretation of $v_{xc}(r)$. On Hartree-Fock approach it represents the exchange interaction on the monoelectronic Fock operator and directly depends on the spin-orbitals χ_i while on Kohn-Sham it represents all kind of electronic interaction, being independently of the spin-orbitals. We can say that on HF we solve a exact Hamiltonian for an approximated wavefunction while on DFT we solve an approximate Hamiltonian (uncertainty on $v_{xc}(r)$) for a exact wavefunction. Developments on the HF methods intend to improve the wavefunction and developments on DFT search a more accurate expression for the exchange and correlation energy. The exchange and correlation energy $E_{xc}[\rho]$ can be expressed as a sum of two contributions

$$E_{xc}[\rho] = E_x[\rho] + E_{corr}[\rho] \tag{46}$$

On the Local Density Approximation (LDA), where the electronic density is associated to an electron uniform gas, the exchange energy, obtained from the result obtained by Block and elaborated by Dirac on the ambit of the Thomas Fermi model, has the expression

$$E_x(\rho) = -C_x \rho(r)^{1/3} \tag{47}$$

with $C_x = \frac{3}{4}\left(\frac{3}{\pi}\right)^{1/3}$, from which the exchange potential comes as

$$v_x^{LDA}[\rho] = -\left(\frac{3}{\pi}\right)^{1/3} \rho(r)^{1/3} \tag{48}$$

The use of this potential with general interest is historically approved from the method X_α developed by Slater on the Hartree Fock method where the potential X_α introduced on the exchange potential has the form:

$$v_{x\alpha}[\rho] = -\frac{3}{2}\alpha\left(\frac{3}{\pi}\right)^{1/3} \rho(r)^{1/3} \tag{49}$$

For $\alpha = 2/3$ this potential corresponds to $v_{xc}^{LDA}[\rho]$. The X_α method is an approximation of the local density that doesn't take in consideration some electronic correlation. In what concerns the form of $E_{corr}[\rho]$ on the ambit of LDA a precious contribution was given by accurate Monte Carlo calculations by Ceperley e Alder who furnished data from which Vosko, Wilk e Nusair (VWN) have extrapolated analytical form for $\varepsilon_{corr}[\rho]$. The LDA approximation is particularly useful for calculation of geometric structures, molecular vibrations, bond and barriers energies. However its only useful for systems where the density changes gradually and not for systems where the density distinguishes very much from the uniform electron gas. For these systems is necessary to leave the idea of of homogeneous density and to introduce the concept of density gradient. On the Generalized Gradient Approximation (GGA) the exchange and correlation energy $E_{xc}[\rho]$ is a functional not only on the density but also on its gradients:

$$E_{xc}^{GGA}[\rho] = \int \varepsilon_{xc}(\rho, |\nabla\rho|, \nabla^2\rho) d^3r \tag{50}$$

Kohn and sham proposed to use the LDA aprximation as the first term of a Taylor expansion for $E_{xc}[\rho]$ (an expansion around the the uniform density) and to add the others term of the series. This new approximation is known as Gradient Expansion Approximation (GEA) doesn't have appreciable practical use but it was fundamental for the construction of several kinds of exchange and correlation

functionals: a) the the Perdew and Wang functional (PW86), useful for guaranteeing the normalization of the exchange functional, b) the correlation functional developed by Perdew, c) the one derivated by Lee, Yang e Parr **(**LYP), based on the approximation of Helium correlation energy proposed by Colle and Salvetti, d) the one developed by Becke (B88) for correcting GEA approximation and e) the ne proposed by Perdew e Wang at 1991 (PW91).

The hybrid functional are currently used in computational chemistry. They mix the exact exchange energy obtained by the Hartree Fock method with e exchange and correlation energies E_x and E_c obtained with the Gradient Approximation method. An example is the the functional PBE0(also named PBE1PBE) developed by Perdew, Ernzerhof and Burcke at 1996. These authors proposed a functional whitut introducing emprical parameters in which the contribution of the exact exchange energy is 25% based on perturbative arguments:

$$E_{xc}^{ibrido} = E_{xc}^{GGA} + 0.25\left(E_x^{HF} - E_x^{GGA}\right) \qquad (51)$$

Bibliography

L. H. Thomas, *Proc. Cambridge Phil. Soc.* **23**, 542 (1926).

E. Fermi, Z., *Phys.* **48**, 542 (1926).

M. Born, J. R. Oppenheimer, *Ann. Phys.*, **84**, 457 (1927).

D.R. Hartree, *Proc.Camb.Phil.Soc.* **24**, 111 (1928).

P. Hohenberg, W. Kohn, *Phys. Rev.*, **136**, B864 (1964).

R. G. Parr, W. Yang in *Density Functional Theory of Atoms and Molecules*, Oxford Univ. Press., New York (1989).

W. Kohn, L. J. Sham, *Phys. Rev.* **145**, 561 (1966).

M. Levy, *Adv.Quant.Chem.* **21**, 71 (1990).

P. A. M. Dirac, *Proc. Cambridge Phil. Soc.* **26**, 376 (1930).

J. C. Slater, *Phys. Rev.*, **81**, 385 (1951).

D. M. Ceperley, *Phys. Rev. B*, **18**, 3126 (1978).

D. M. Ceperley, B. J. Alder, *Phys. Rev. Lett.*, **45**, 566 (1980).

S. H. Vosko, L. Wilk, M. Nusair, *Can. J. Phys.*, **58**, 1200 (1980).

W. Kohn, L. J. Sham, *Phys. Rev. A*, **140**, 1133 (1965).

J. P. Perdew, Y. Wang, *Phys. Rev. B*, **33**, 8800 (1986); **34**, 7406(E) (1986).

J. P. Perdew, *Phys. Rev. B*, **33**, 8822 (1986).

C. Lee, W. Yang, R. G. Parr, *Phys. Rev. B*, **37**, 785 (1988).

R. Colle, D. Salvetti, *Theor. Chim. Acta*, **37**, 329 (1975).

R. Colle, D. Salvetti, *J. Chem. Phys.*, **79**, 1404 (1983) .

A. D. Becke, *Phys. Rev. A*, **38**, 3098 (1988).

J. P. Perdew, *Phys. Rev.* B, **44**, 10221 (1991).

J. P. Perdew, Y. Wang, *Phys. Rev.*, **45**, 13244 (1992).

J. P. Perdew, M. Ernzerhof, K. Burke, *J. Chem. Phys.*, **105**, 9982 (1996).

K. Burke, M. Ernzerhof, J. P. Perdew, *Chem. Phys. Lett.*, **265**, 115 (1997).

J. P. Perdew, M. Ernzerhof, K. Burke, *Phys. Rev. Lett.*, **77**, 3865, (1996); Erratum, *ibid.*, **78**, 1396 (1997).

M. E. Casida, In *Recent Advances in Density Functional Methods, Part I*; Chong, D. P., Ed.; Word Scientific: Singapore, 1995.

E. Runge, E. K. U. Gross, *Phys. Rev. Lett.k*, **52**, 997 (1984).

E. K. U. Gross, E. Runge, *Phys. Rev. Lett.*, 55, 2850 (1985); Erratum, *ibid.*, 57, 923 (1985).

4) Expanded porphyrins

Porphyrin frameworks consists of four pyrrole subunits that are connected in a coplanar fashion at their α-carbon atoms through a methine carbon bridge. Most porphyrins exist as a conjugated 18π electronic aromatic circuit. Porphyrin like molecules (figure 1) have a strong versatility on their structure and on living beings they are involved on diverse important functional activities.

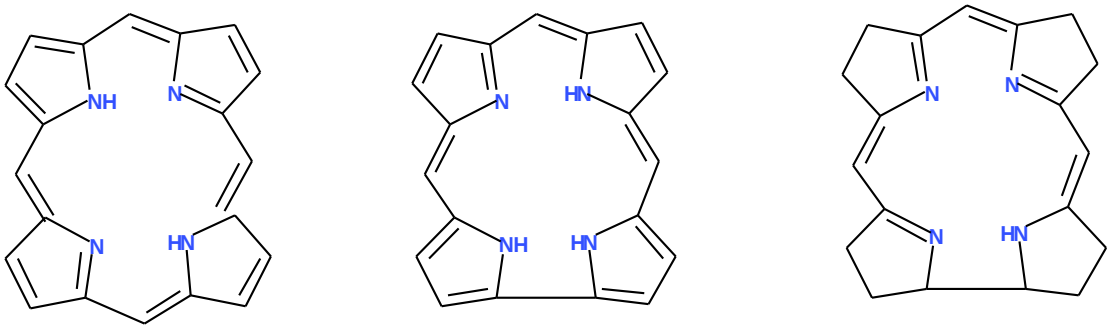

porphyrin **corrole** **corrin**

Figure1

On plant and bacterial cells the green pigment Chlorophylls, a Mg (II)-chlorin complex, with other pigments constitute the supra molecular units called photosystems I and II that possess the functions of absorbing and transferring light energy on the process of solar energy capture named photosynthesis. On the vertebrate erythrocytes, the heme, a red Fe (II)-protoporphyrin complex group, is part of the protein hemoglobin and has oxygen carrying functions. A very important vitamin for the maturation of erythrocytes is vitamin B_{12}, a Co(II)-corrin complex, that has the particularity of not being produced by the animal cells but being absorbed in diet.

Expanded porphyrins are porphyrin like compounds containing more than four pyrrole rings and these rings are connected by one or more methine carbon bridges (figure 2) that gives them rich chemical properties such as the versatile ways of connecting pyrrole rings to produce a variety of expanded porphyrin and multiple conformational changes and very importantly, the resulting larger cavity comparing to the porphyrin, given the capacity of these compounds to chelate almost all the metal of the periodic table.

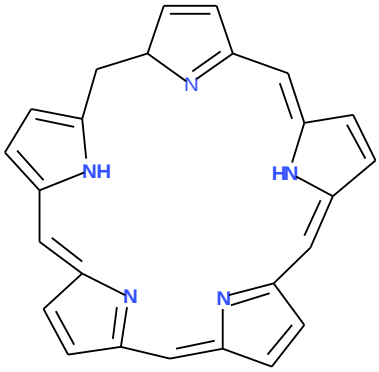

pentaphyrin

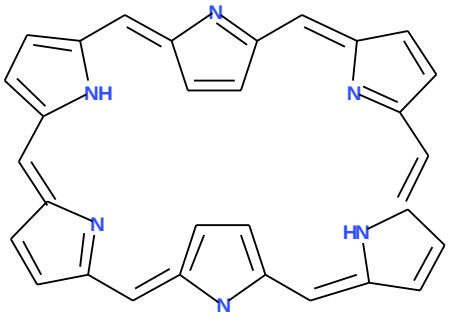

hexaphyrin

Figure 2

The systematic nomenclature of porphyrin analogues, as proposed by Franck and Nonn [1],is useful for expanded porphyrins. In this nomenclature, a name of an expanded porphyrin is built by specifying the number π electrons in the effective macrocyclic conjugation, a name for the number of pyrrole rings, e.g. pentaphyrin, hexaphyrin for expanded porphyrins consisting of five and six pyrrolic subunits, and by the numbers of bridging carbon atoms between the constitutional pyrrole groups, starting from the largest unit.

According to this nomenclature, porphyrin and hexaphyrin are named as [18]porphyrin (1.1.1.1) and [26]hexaphyrin(1.1.1.1.1.1), respectively. Some expanded porphyrins are named after their colors, which include sapphyrin for [22]pentaphyrin(1.1.1.1.0) , amethyrin for [24]hexaphyrin(1.0.0.1.0.0) and rubyrin for [26]hexaphyrin(1.1.0.1.1.0).

The chemistry of expanded porphyrins started after the discovery of sapphyrin (figure 3) by Woodward et al. in 1966 although the full report of the discovery was published only in 1983 [ref 2].

It is a 22π electron pentapyrrolic macrocycle that forms a dark blue solid which exhibits an intense Sore t like band at 450 nm ($CHCl_3$) along with weaker Q-type transitions in the 620-690nm region. These optical properties along with the presence of a large central cavity, which could possibly serve for metal binding, suggested that sapphyrin and its derivatives might find use in a variety of emerging biomedical applications, notably in photodynamic therapy (PDT) where long wavelength (2680 nm) absorptions are desired, and in magnetic resonance imaging enhancement (MRI) where chelation of highly paramagnetic metal cations such as gadolinium(III) would be particularly worthwhile.

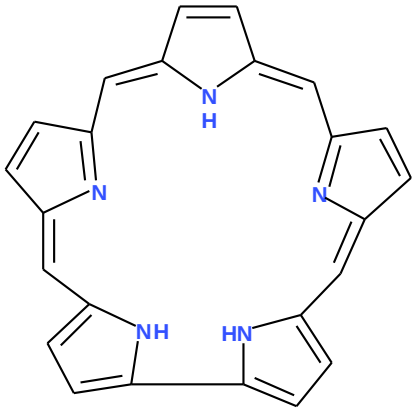

Figure 3

However for Osuka et al [3], the renaissance of expanded porphyrins is largely due to Sessler and co-workers, who reported texaphyrin (figure 4) in 1988,[4] and on the improved synthesis of sapphyrin in 1990 [5].

The first work of Sessler et al [4] reported the synthesis of a non aromatic methylene bridged pentaphyrin instead of methine bridged, named texaphyrin. They found that stirring this reduced macrocycle with cadmium chloride which gave the oxidized cadmium complex with Cl as ligand (figure 4) that meant simultaneously oxidation and metal complexation have occurred. The metal complex contains a 22 π electron conjugation system while the parent compound contains only 18 π. In addition to the Soret band this metal complex presents a Q band at 767.5 nm which is substantially red shifted (200 nm) as compared to that of typical cadmium porphyrin complex.

Later Sesslet et al[6] demonstrated the potential of these expanded porphyrins on the field of anion recognition. During that time, Sessler and co-workers were working to develop a more efficient synthesis of sapphyrin. However, the X-ray structure of the compound of this work,solved by Ibers and McGhee, revealed the presence of electron density in the center of the pentapyrrolic macrocycle that on the basis of independent synthesis and ^{19}F-NMR spectroscopic analyses, was ascribed to a fluoride counter anion bound within the protonated core (figure 5) .

Young et al [7], from the Seesler's group reported the synthesis a Lutetium texaphyrin complex, Lu-tex, (figure 6) to be used on Photodynamic Therapy with the aim to overpass some the well known problems inherent to the approved drug PHOROFRIN. The most important feature of Lu-Tex is that it is water soluble and easy to administer via intravenous injection.

In contradiction to PHOTOFRIN, it is also a single unique compound that possesses the lowest energy maximum at 732 nm in the far-red portion of the visible spectrum where blood and bodily tissues are most transparent.

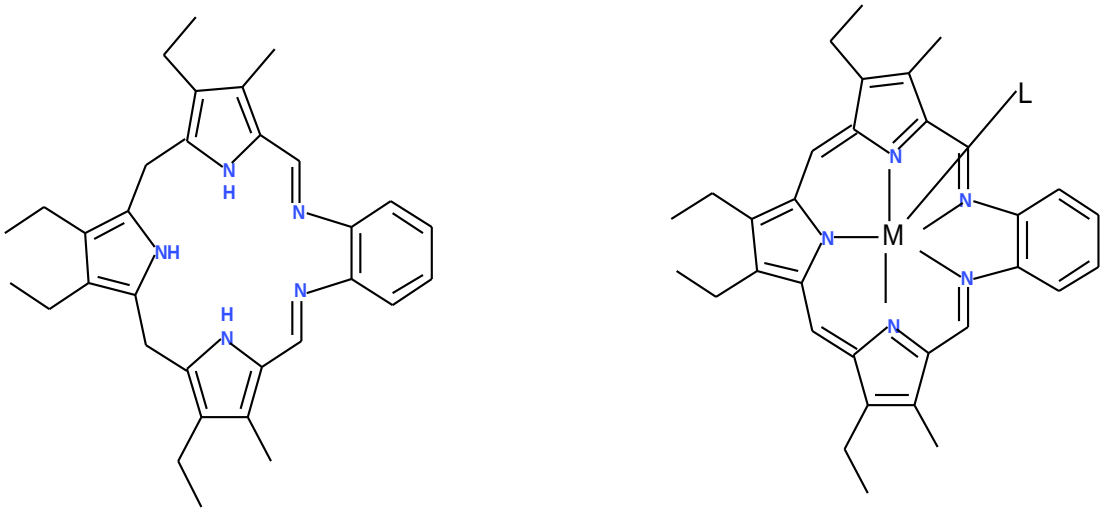

reduced texaphyrin free base **texaphyrin**

Figure 4

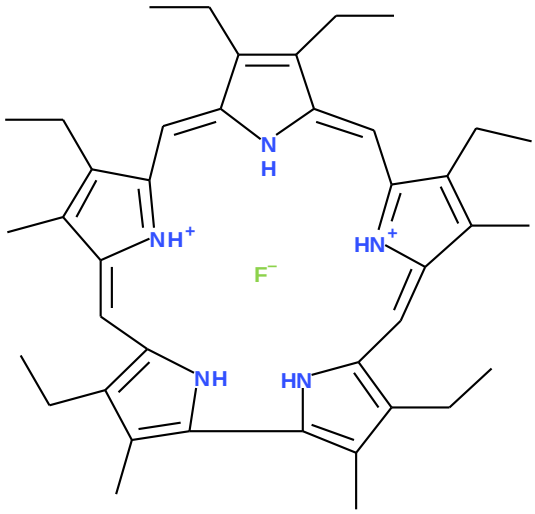

Figure 5

Being diamagnetic and containing a heavy atom (lutetium), it also produces singlet oxygen in good quantum yield (between 10 and 70 %, depending on conditions) when irradiated at this lowest energy maximum.

Furthermore, Lu-Tex exhibits low dark toxicity, which is related primarily to its more rapid plasma clearance. Specifically in humans, this agent is cleared on a time scale that is measured in hours, whereas PHOTOFRIN is cleared on a time scale that is measured in months. The more rapid clearance of Lu-Tex is likely responsible for its reduced cutaneous phototoxicity as compared to PHOTOFRIN. Nonetheless, in spite of its relatively rapid clearance, it is still retained selectively in neoplastic sites as well in macrophages in the body.

LUTRIN injection is the Lu-Tex drug formulation being developed for use as a photosensitizer in PDT treatment of cancer. LUTRIN also was found to be active in a Phase I clinical study for the treatment of metastatic tumors of the skin and subcutaneous tissues and was the subject of a recently completed Phase II clinical trial for recurrent breast cancer to the chest wall.

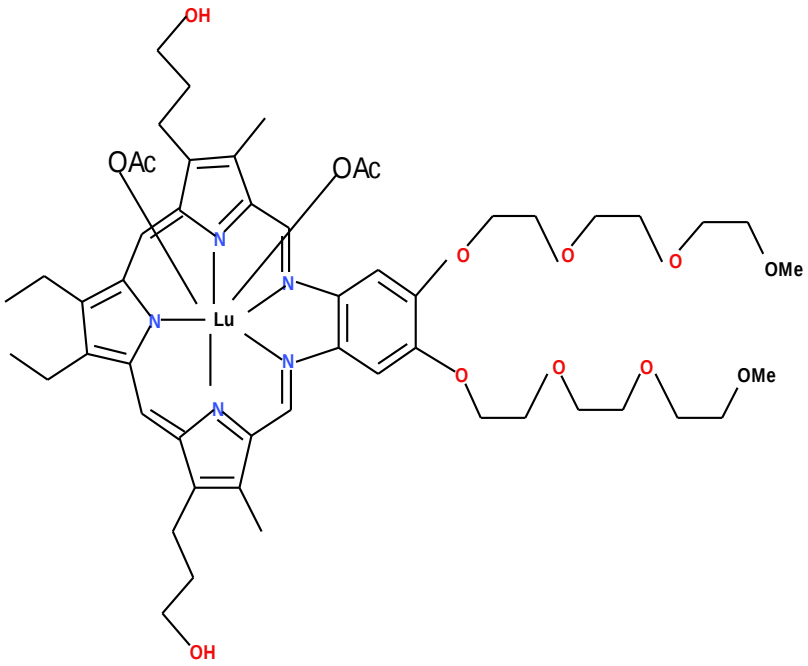

Figure 6

Recently, Ballico et al[8] reported the synthesis and cytotoxic activity of two new macrocycles belonging to the class of [1.1.1.1.1]-pentaphyrins and its Lu(III)-complex, respectively, compounds 1 and 2 on figure (figure 7).

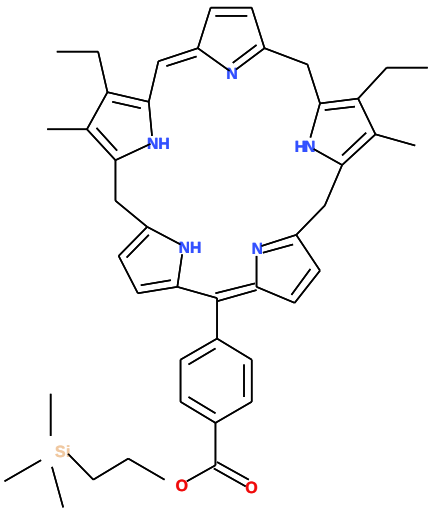

pentaphyrin

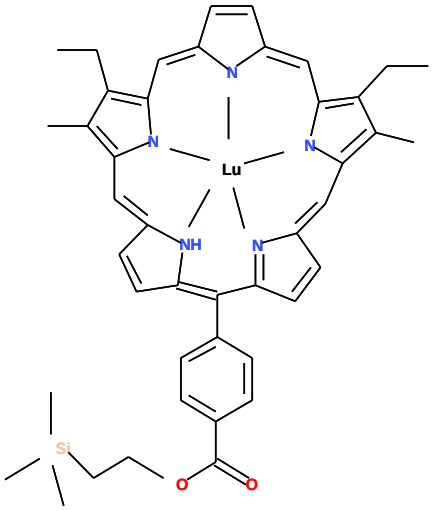

Lu-pentaphyrin

Figure 7

Bibliography

[1] Franck B, Nonn A (1995)

Novel Porphyrinoids for chemistry and medicine by biomimetic syntheses

ANGEWANDTE Chemie International Edition Vol 34, Issue 17, 1795-1811

[2] Bauer VJ, Clive DLJ, Dolphin D

Sapphyrins: novel aromatic pentapyrrolic macrocycls

Journal of the American Chemical Society, Vol 105, Issue 21, 6429-6436

[3] Saito S, Osuka A (2011)

Expanded Porphyrins: Intriguing Structures, Electronic Properties, and Reactivities

ANGEWANDTE Chemie International Edition, Vol 50, Issue 19, 4342-4347

[4] Sessler JL, Murai T, Lynch V e al (1988)

An expanded porphyrin – the synthesis and structure of a new aromatic pentadentate ligand

Journal of the American Chemical Society, Vol 110, Issue 16, 5586-5588

[5] Sessler JL, Cyr MJ, Lynch V et al (1990)

Synthetic and structural studies of Sapphyrin, a 22 π electron pentapyrrolic expanded porphyrin

Journal of the American Chemical Society, Vol 112, Issue 7, 2810-2813

[6] Sessler JL, Camiolo S, Gale PA (2003)

Pyrrolic and polypyrrolic anion binding agents

Coordination Chemistry Reviews, Vol 240, Issue 1-2, 17-55

[7] Young SW, Woodburn et al (1996)

Lutetium texaphyrin (PCI-0123): A near-infrared, water-soluble photosensitizer

Photochemistry and Photobiology, Vol 63, Issue 6, 892-897

[8] Ballico M, Rapozzi V, Xodo LE and Comuzzi C (2011)

Metallation of pentaphyrin with Lu(III) dramatically increases reactive-oxygen species production and cell phototoxicity

European Journal of Medicinal Chemistry, Vol 46, Issue 2, 712-720

THE JOURNAL OF PHYSICAL CHEMISTRY B

Article

pubs.acs.org/JPCB

A Time-Dependent Density Functional Study of a Non-Aromatic [1.1.1.1.1]-Pentaphyrin and Its Lutetium Complex

Flavio Fortes Ramos Sousa, Angelo Domenico Quartarolo, Emilia Sicilia, and Nino Russo*

Dipartimento di Chimica and Centro di Calcolo ad Alte Prestazioni per Elaborazioni Parallele e Distribuite-Centro di Eccellenza MIUR, Università della Calabria, I-87030 Arcavacata di Rende, Italy

Supporting Information

ABSTRACT: The molecular structures and absorption electronic spectra of two novel phototoxic pentapyrrolic expanded porphyrins (a isopentaphyrin derivative and its lutetium complex) have been studied at the density functional level and its time-dependent extension (TDDFT). The geometries were optimized with three different exchange-correlation functionals (PBE0, B3LYP, and ωB97XD) and the SV(P) basis set plus the pseudopotential method for the complex. With respect to the porphyrin, the structure of [1.1.1.1.1]-pentaphyrin and its lutetium complex are predicted much distorted due to the lack of conjugation. The lowest excitation energy band (experimental at 814 nm) for the free-base isopentaphyrin is well predicted by the ωB97XD at 772 nm. The possible photodynamic reaction mechanisms (types I and II) were studied through the calculation of the electron affinity and ionization potentials in solvent, using the COSMO model.

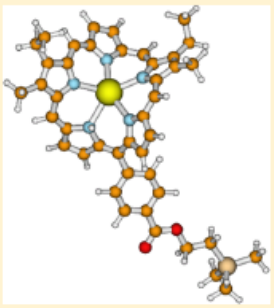

1. INTRODUCTION

Tetrapyrrolic macrocycles are a porphyrin-like class of compounds where the pyrrole rings are held together through *meso*-methine carbon bridges, in a square-planar geometry.[1] The metal-complex form of porphyrins plays a crucial role in many biological processes of life chemistry.[2] Chlorophylls (Mg(II)-chlorin), vitamin B-12 (Co(II)-corrin), and heme (Fe(II)-protoporphyrin) are natural porphyrin complexes essential for plant photosynthesis, oxygen transport in blood, electron transport, and redox catalysis. The spectral features of porphyrins are essentially due to the π-electron conjugation that causes the appearance of absorbing bands in the visible region (400−700 nm).[3] The extension of the macrocycle cavity size with the inclusion of more than four pyrrole subunits brings a new class of polypyrrolic chromophores termed expanded porphyrins.[4,5] The first expanded porphyrin, discovered by Woodward et al. in 1966 but reported with a full characterization only in 1983, was the sapphyrin, a pentapyrrolic macrocycle, whose name was assigned from its color.[6,7] A more general definition of expanded porphyrins, due to Sessler et al., implies the presence of heteroatom rings (thiophene, pyrrole, or furan-like) bonded directly or not through spacers, with at least 17 atoms in the main ring pathway.[8] The nomenclature proposed by Frank and Nonn consists of three parts: (a) the number of π electrons as a prefix in square-brackets; (b) the number of pyrrole units (e.g., pentaphyrin, hexaphyrin); (c) the number of bridging carbons between heteroatom rings in round-brackets.[9] The molecule reported in Figure 1, for example, belongs to the [24] pentaphyrin (1.1.1.1.1) class. The importance of the expanded porphyrins has emerged in different application fields: as photosensitizers in photodynamic therapy (PDT), nonlinear optical materials with large TPA cross sections, near-infrared dyes, contrast agents in magnetic resonance imaging (MRI), and anion recognition sensors.[10−13] The absorption spectra of the expanded porphyrins are generally bathochromically red-shifted with respect to porphyrins because of the increase of the π-electron conjugation length.[4] The enlargement of the inner cavity allows the metal coordination to larger cation ions, than in porphyrins, like lanthanides or actinides.[14] This is the case for the lutetium(III) and gadolinium(III) water-soluble texaphyrin complexes (tripyrrolic penta-aza expanded porphyrins), first synthesized by Sessler et al. in 1993, with a cavity core larger by about 20% than that of porphyrins.[15] These metal complexes are in advanced clinical studies for the PDT treatment of arteriosclerotic disease and as MRI radiation enhancers, respectively. PDT is a light-assisted treatment of tissue lesions and tumors, in which, schematically, a photosensitizer is excited from its ground state S_0 to the first excited state S_1 and then through a radiationless intersystem crossing transition generating the T_1 triplet excited state.[16,17] The electron energy transfer to molecular oxygen ($^3O_2$) can generate the cytotoxic singlet oxygen ($^1O_2$) species (type II PDT mechanism). Another proposed photodynamic action mechanism (type I) is based on the reduction of the photosensitizer in its T_1 state by an organic substrate. The subsequent reaction with $^3O_2$ generates the reactive oxygen species (ROS).[18] The presence of absorption bands, in the so-called therapeutic window (650−800 nm), and the heavy atom in the macrocycle represent some important photochemical features for the design of suitable PDT photosensitizers. In fact, in the first case (red-shifted bands), the radiation allows the treatment of deeper tumors and in the second case (heavy atom presence) the triplet quantum yield can increase because of the intersystem spin

Received: July 10, 2012
Revised: July 31, 2012
Published: August 9, 2012

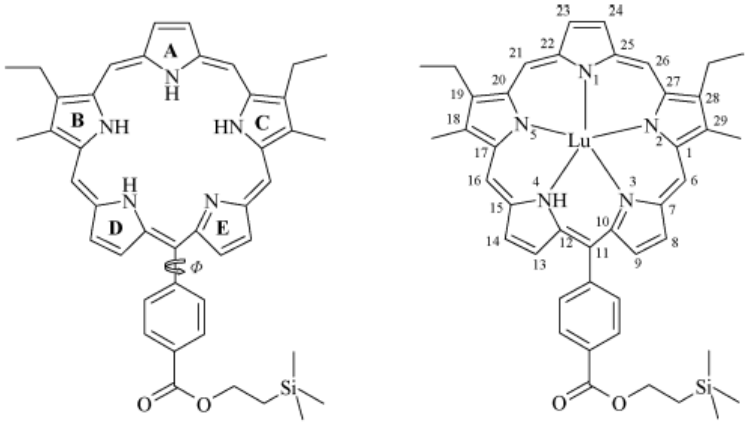

Figure 1. Molecular structures for the isopentaphyrin (1) and the lutetium complex (2), with atom numbering and ring labeling.

crossing.[19] Recently, the synthesis of a non-aromatic free base expanded pentaphyrin, or 20-[4′-(trimethylsilyl)ethoxycarbonyl]phenyl-2,13-dimethyl-3,12-diethyl-[24] iso-pentaphyrin, its zinc(II) and lutetium(III) complexes have been reported for potential application in PDT.[20] In particular, the lutetium complex showed a great ROS production and phototoxicity in several cancer line cells. In the present theoretical work, we will deal with the ground and excited state properties of these compounds, at the density functional level of theory and its time-dependent formalism, in order to calculate the electronic spectra and characterize their spectral features. Moreover, the basic PDT mechanisms will be investigated, by means of the excited state electron affinities and ionization potential calculations.

2. COMPUTATIONAL DETAILS

Molecular geometry optimization of **1** and **2** structures, in the ground singlet and excited triplet electronic states, was carried out without symmetry constraints at the density functional level of theory. For this purpose, two different kinds of exchange-correlation functionals, belonging to the pure hybrid (a) and long-range corrected hybrid (b) models, were employed: (a) the Becke semiempirical three-parameter gradient corrected (B3LYP)[21] and the parameter-free Perdew−Burke−Erzenrhof (PBE0);[22,23] (b) the ωB97X and ωB97XD functionals.[24,25] The B3LYP and PBE0 functionals contain different amounts of the Hartree−Fock (HF) exact exchange energy (20 and 25%, respectively). The performance of the B3LYP and PBE0 approaches, for the prediction of molecular geometries and optical properties, is well established in the literature, for the study of the ground and excited states of organic and metal-containing systems.[26,27] For the molecular optimizations, the SV(P) split-valence basis set of Ahlrichs et al. was used, which includes polarization functions on C, N, O, and Si atoms.[28] The Stuttgart pseudopotential (SDD) was used for the lutetium atom (including 60 core electrons), with the optimized valence basis set taken from ref 29. The vibrational analysis, carried out on the optimized structures, has given all real eigenvalues for the Hessian matrix. Electronic absorption spectra were calculated by means of the time-dependent DFT formalism[30] at the corresponding ωB97X(D) optimized geometries. For the ωB97X(D) long-range corrected hybrid functional, the Coulomb term (r_{12}^{-1}) is split into a short- and long-range (with about 16 and 100% of exact exchange, respectively). It has been shown that the application of this functional improves, against the hybrid B3LYP and meta-hybrid (e.g., M06) functionals, the description of the low-lying electronic excitation energies for different tetrapyrrolic derivatives (e.g., porphyrin, chlorin).[31,32] The bulk solvent effects on excitation energies were treated within the conductor-like screening solvation model (COSMO).[33] The dielectric constant of dichloromethane (ε = 8.93) was set up along with the default cavity generation parameters. The more extended def2-SVP basis set,[34] including diffuse functions for H, C, N, O, and Si atoms, was employed for the calculation of the *in vacuo* and solution (dichloromethane and water) vertical electron affinities (VEA) and ionization potentials (IP), at the gas-phase B3LYP and PBE0 optimized geometries. The quantum-chemical calculations were carried out by means of the TURBOMOLE (for the B3LYP and PBE0 functionals) and Gaussian 03 (ωB97X and ωB97XD functionals) software packages.[35,36]

3. RESULTS AND DISCUSSION

3.1. Gas-Phase Optimized Structures. The molecular structures of the free-base iso-pentaphyrin (**1**) and its lutetium complex (**2**) have been experimentally characterized by different spectroscopic techniques (^{1}H NMR, 2D COSY, and UV−vis spectra), and their stoichiometric formulas were deduced from the mass spectrometry (ESI-MS and EI).[20] Our starting geometry follows the proposed structures by Comuzzi et al. and is reported in Figure 1. Selected optimized geometrical parameters (bond lengths and valence and torsional angles) for both **1** and **2** molecules are reported in Table 1. Their optimized structures display a highly distorted conformation, as can be shown from the dihedral angle values (Table 1) between adjacent pyrrolic rings (labeled A−E in Figure 1b). For the free base, the PBE0 torsional angle values range between 22 and 38°, with the exception of the dihedral Φ(C−E) that is about 4°. The structural differences among each functional (PBE0, B3LYP, and ωB97X) are very small, also including the sp^2 methine bridged valence angles (e.g., $C_{20}-C_{21}-C_{22}$) and the torsional angle Φ around the atom C_{11} and the substituted phenyl group. The latter Φ(C_{11}-phenyl) angle rotated by about 60°. The optimized geometrical parameters for the ωB97XD are also included in Table 1 for compound 1, and they are almost identical to the ωB97X values. For the lutetium complex (**2**), the Lu−N bond lengths are shorter for N_1-N_3 and N_5 atoms (PBE0 results: 2.272−2.381 Å)

Table 1. Main Bond Lengths (Å), Valence and Dihedral Angles (deg) for the Lutetium Complex (2) and, in Parentheses, for the iso-Pentaphyrin Free-Base Derivative (1), Calculated at the PBE0, B3LYP, and ωB97X Levels of Theories

	PBE0	B3LYP	ωB97X
		Bond Lengths	
Lu−N_1	2.272	2.278	2.292
Lu−N_2	2.311	2.333	2.332
Lu−N_3	2.329	2.304	2.398
Lu−N_4	2.525	2.601	2.533
Lu−N_5	2.381	2.411	2.340
		Valence Angles	
C_{20}−C_{21}−C_{22}	127.9 (128.8)	128.6 (128.4)	128.1 (126.3) [126.6][a]
C_{34}−C_{26}−C_{27}	121.0 (128.4)	122.9 (131.1)	120.2 (127.2) [126.8]
C_{15}−C_{16}−C_{17}	125.6 (131.8)	126.8 (128.8)	125.9 (129.4) [129.4]
C_1−C_6−C_7	125.7 (130.2)	126.3 (128.7)	126.1 (130.0) [129.4]
C_{10}−C_{11}−C_{12}	120.5 (123.2)	119.7 (124.9)	120.8 (122.9) [123.0]
N_1−Lu−N_5	81.0	82.6	81.1
N_1−Lu−N_2	75.5	76.6	75.1
N_4−Lu−N_5	74.9	74.8	75.0
N_2−Lu−N_3	75.9	75.7	75.5
N_4−Lu−N_3	68.9	67.0	68.9
		Dihedral Angles	
Φ(C_{11}-phenyl)	48.6 (59.9)	51.3 (60.8)	52.9 (61.4) [62.0]
Φ(A-B)	25.7 (36.6)	27.1 (36.3)	25.8 (45.7)
Φ(A-C)	9.3 (29.2)	13.3 (30.6)	8.8 (31.6)
Φ(B-D)	42.0 (38.4)	39.1 (41.7)	41.2 (48.3)
Φ(C-E)	5.3 (3.8)	0.9 (10.7)	4.3 (3.2)
Φ(D-E)	32.6 (22.4)	28.2 (17.5)	31.5 (25.0)

[a]In square brackets are reported selected valence and dihedral angle values calculated at the ωB97XD/SV(P) level for compound 1.

and slightly longer for Lu−N_4 (2.525 Å). The same trend is found for the B3LYP and ωB97X optimized geometries. For compound 2, since the ωB97XD functional is not parametrized for lutetium atom, the optimization of this structure is not possible at this level of theory. The metal coordination lengths with the atoms N_1−N_3 are significantly reduced, with respect to the free base (1), the torsional angles between the corresponding pyrrolic rings are Φ(A−B) and Φ(A−C). The agreement between the computed and experimental structural parameters is quite satisfactory.

The natural atomic population and charges, derived from the NBO wave function analysis at the PBE0 level of theory, are reported in Table 2 and give some hints about the metal to ligand bond character. For the lutetium atom, the used pseudopotential assigns a $5s^2 5p^6 5d^1 6p^2$ ground-state valence configuration with 14 electrons in the f-core shell. Considering the lutetium atom in a formal charge of +3, the calculated f-orbital and d-orbital metal occupation numbers and their natural charge are 0.00, 0.48, and 2.36, respectively. This indicates a covalent metal−nitrogen bonding character, due to the partial electron donation from the pyrrolic nitrogens, whose calculated atomic charges are about −0.8. The PBE0 optimized Cartesian coordinates for compounds 1 and 2 are given in the Supporting Information.

3.2. Electronic Absorption Spectra. The spectra of porphyrins are usually rationalized through the four-orbital model proposed by Gouterman.[3,37] Mixed electronic transitions between the two highest occupied (HOMO and HOMO+1) and the two lowest unoccupied (LUMO and LUMO+1) molecular orbitals can explain the main spectroscopic features of the electronic absorption bands: the B or Soret bands (B_x and B_y) in the near-UV region and the weaker intensity Q-bands (Q_x and Q_y) in the visible or near-IR spectrum region. For expanded aromatic porphyrins, the electronic spectra similarly exhibit the strong allowed Soret band and several distinct Q-bands in the near-IR region.[4,38] The increased macrocycle size causes the bathochromic wavelength red-shift of the Q-band absorption maxima because of the π-electron delocalization. This effect is generally not linear with the number of pyrrole rings, since the structures tend to deviate from planarity and become more hindered, decreasing the electronic conjugation. The spectral features of expanded aromatic porphyrins (distinct B and Q-bands) are not present in non- or antiaromatic congeners.[39] The electronic spectrum of [24]amethyrin (an hexapyrrolic expanded porphyrin) is a representative example for this behavior showing broad absorption maxima without distinct Q-bands in the near-infrared region.[38] In this case, the electronic spectrum appearance can also be taken as a qualitative test for assigning them to be antiaromatic or aromatic compounds. The 1 and 2 antiaromatic pentapyrrolic porphyrins, reported in Figure 1, display these spectral features: broad absorption bands and no Q-bands in the near-IR region. In particular, the experimental spectrum of 1 recorded in dichloromethane solution (CH_2Cl_2) has a Soret-like band centered at 485 nm (2.56 eV, $\log \varepsilon = 4.39$) and a broad Q-band absorption wavelength maximum (λ_{max}) at 814 nm (1.52 eV, $\log \varepsilon = 3.71$).[20] The computed five lowest excitation energies, oscillator strengths, and main orbital contributions of compound 1 in CH_2Cl_2 are reported in Table 3. Since the first excitation energy (Q-band) is predicted at very low energy for both B3LYP and PBE0 exchange-correlation functionals (λ_{max} = 1340 and 1501 nm, respectively), the reported data refer to the ωB97X and ωB97XD functionals. In this case, the lowest excitation energies are found at 1.95 eV (636 nm) and 1.61 eV (770 nm), slightly overestimated in comparison with the experimental values. For the ωB97XD, the agreement with the experimental Q-band is better and smaller than 0.1 eV, though the oscillator strength is slightly weaker in comparison with the ωB97X value (0.02 vs 0.06). The Q-band absorption peak is mostly dominated by the HOMO−LUMO electronic transition with orbital contributions changing from 87% (for ωB97X) to 93% (for ωB97XD). The isodensity molecular surface plots for the most contributing molecular orbitals to

Table 2. NBO Atomic Orbital Populations (s, p, d, and f) and Atomic Charges for Lutetium and Nitrogen Atoms for Complex 2 and iso-Pentaphyrin 1 (in Parentheses), Calculated at the PBE0/SV(P) and Stuttgart Pseudopotential Level of Theory

	s		p		d		f	charge	
Lu	2.18		6.01		0.46		0.00	2.36	
N1	3.35	(3.37)	4.50	(4.24)	0.00	(0.01)	0.00	−0.86	(−0.63)
N2	3.34	(3.22)	4.47	(4.34)	0.00	(0.00)	0.00	−0.81	(−0.56)
N3	3.35	(3.37)	4.44	(4.24)	0.00	(0.01)	0.00	−0.80	(−0.62)
N4	3.32	(3.22)	4.45	(4.39)	0.00	(0.00)	0.00	−0.78	(−0.61
N5	3.36	(3.22)	4.46	(4.33)	0.00	(0.00)	0.00	−0.82	(−0.56)

Table 3. Five Lowest Excitation Energies ΔE (eV, nm), Main Configurations, and Oscillator Strengths f for Compound **1**, Calculated at the ωB97X and ωB97XD/SV(P) Levels, and for Compound **2**, Calculated at ωB97X/SV(P) and Stuttgart Pseudopotential[a]

	TD-ωB97X			TD-ωB97XD		
n	$\Delta E^{b,d}$ (eV, nm)	configuration[c]	f	ΔE^{b} (eV, nm)	configuration[c]	f
			Compound 1			
1	1.95, 636	H → L (87)	0.064	1.61, 772	H → L (93)	0.027
2	3.34, 371	H − 1 → L (44) H → L + 1 (35)	1.939	3.13, 396	H → L + 1 (48) H − 1 → L (29) H − 2 → L (11)	1.897
3	3.42, 362	H → L + 2 (58) H − 2 → L (29)	1.563	3.18, 389	H → L + 2 (66) H − 2 → L (15) H − 1 → L (11)	1.400
4	3.89, 319	H → L + 1 (39) H − 1 → L (34)	0.143	3.43, 361	H − 1 → L (40) H → L + 1 (32) H − 2 → L (11)	0.079
5	4.05, 306	H − 2 → L (54) H → L + 2(26)	0.036	3.54, 350	H − 2 → L (57) H → L + 2 (21) H − 1 → L (13)	0.107
			Compound 2			
1	1.51, 820	H → L (92)	0.023			
2	3.06, 406	H → L + 1 (51) H − 2 → L (19)	1.375			
3	3.19, 389	H − 1 → L (56) H → L + 2 (24)	1.110			
4	3.49, 355	H → L + 4 (30) H → L + 6 (26) H → L + 3 (17) H → L + 2 (15)	0.040			
5	3.69, 336	H − 2 → L (50) H → L + 1 (21)	0.061			

[a]Solvent effects were included by means of the COSMO solvation model (ε = 8.93). [b]Experimental absorption peaks in dichloromethane for compound **1**: 485 nm (log ε = 4.39), 814 nm (log ε = 3.71). [c]In parentheses are reported the orbital contributions with the convention that the first number, n, refers to the occupied orbitals (HOMO − n) and the second (m) to the virtuals (LUMO + m). [d]Experimental absorption peaks in dichloromethane for compound **2**: 339 nm (log ε = 4.25), 406 nm (log ε = 4.15), 498 nm (log ε = 3.99).

excitation energies of compound **1** are reported, for the ωB97XD case, in Figure 2. The H → L electronic transition, responsible for the Q-band appearance, has a $\pi \rightarrow \pi^*$ orbital character with the electron density delocalized over all of the isopentaphyrin macrocycle. The experimental Soret-like band shows an absorption maximum at 485 nm (2.56 eV), in the near-UV region. In the case of ωB97X computations, the most intense electronic transitions ($S_0 \rightarrow S_2$ and $S_0 \rightarrow S_3$) contributing to this band are at 371 and 362 nm (f = 1.939 and 1.563), while for the ωB97XD they are found at 396 and 389 nm (f = 1.897 and 1.400). The electronic transitions are mainly made by a mixture of orbital contributions from different molecular frontier orbitals (from H − 2 to L + 2), showing that the Gouterman model is not strictly followed for this class of porphyrinoid molecules. The simulation of the electronic spectrum for compound **1** in CH_2Cl_2 (at ωB97X and ωB97XD theory level) obtained by means of a sum of Gaussian functions is reported in Figure 4 (left side). It takes into account the first 20 excitation energies and the corresponding oscillator strengths with a full width at half-maximum of 0.3 eV. The convoluted absorption peaks of the Soret-like band for the ωB97X and ωB97XD functionals are located at 368 nm (3.37 eV) and 392 nm (3.16 eV), respectively. For the corresponding lutetium(III) metal complex (**2**), the experimental UV−vis band shape in dichloromethane shows three broad absorptions at 339, 406, and 498 nm. The corresponding experimental Soret band pattern gives an absorption maximum at 480 nm. The main computed excitation energies, oscillator strengths, and main configuration, in dichloromethane, are listed in Table 3. For this compound, it was not possible to investigate the ωB97XD functional, since at present it is not parametrized for the lutetium atom. The simulated spectrum of **2** displays some analogies with the metal free molecule. The HOMO−LUMO transition, for the B3LYP and PBE0 calculations, is still present, though very weak ($f \sim 0.004$) and further red-shifted (1750 and 1890 nm) with respect to compound **1**. The corresponding ωB97X first excitation energy is at 820 nm with an oscillator strength of about 0.02, corresponding to a very weak band in the convoluted spectrum (see Figure 4, right side). The absence of the Q-band absorption in the experimental spectrum of compound **2** can be likely ascribed to the shorter lifetime of the S_1 state, enhancing so the radiationless internal conversion between the S_0 and S_1 electronic states. The ωB97X isodensity molecular surface plots for the most contributing molecular orbitals to the excitation energies of **2** are reported in Figure 4. The contribution of the metal center is evident for the L + 1 and L + 2 molecular orbitals. The Soret band stems, as for compound **1**, from the $S_0 \rightarrow S_2$ and $S_0 \rightarrow S_3$ electronic transitions having excitation energies at 3.06 and 3.19 eV, respectively. The convoluted absorption maximum is found at 398 nm (3.11 eV), differing by about 0.5 eV from the experimental value.

3.3. Photosensitization PDT Mechanisms. The combination of light, photosensitizer, and dioxygen can promote two main photochemical reactions with organic substrates (membrane

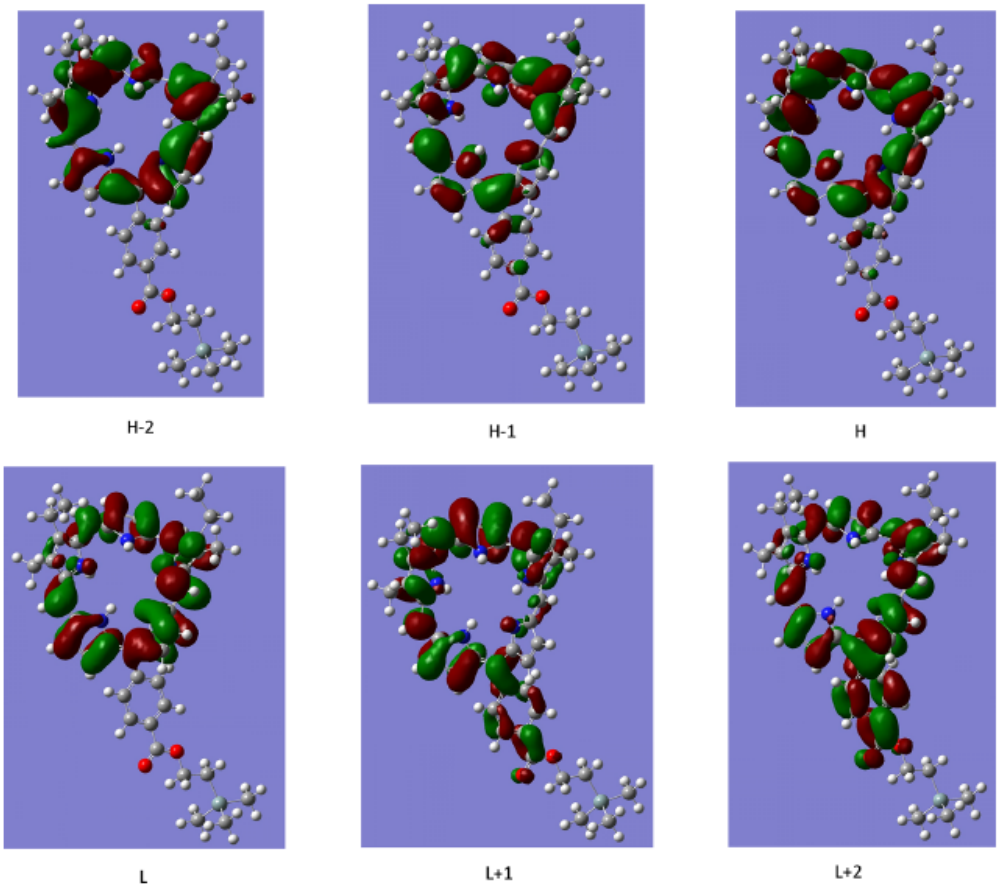

Figure 2. Frontier molecular surface plots (from HOMO − n to LUMO + n) with isodensity value of 0.02 au, for compound **1** calculated at the ωB97XD/SV(P) level of theory and solvent model.

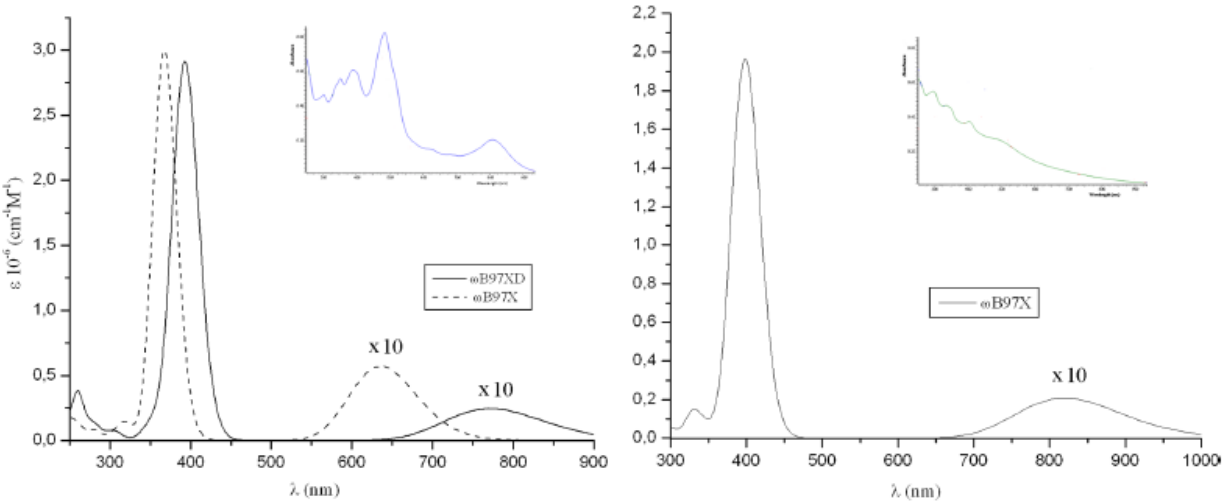

Figure 3. Simulated electronic spectra of compound **1** (left side) calculated at ωB97X/SV(P) (solid line) and ωB97XD/SV(P) (dot line) and compound **2** (right side) at ωB97X/SV(P)/SDD in dichloromethane. The inset shows the experimental spectra.

lipids or DNA nucleic acid bases and eventually cell damage through the generation of reactive oxygen species (ROS)). These processes, called type I and type II reaction mechanisms, will be examined together with the direct electron transfer to dioxygen and the autoionization processes, which can compete with the type I and II reactions.

3.3.1. Type I Mechanism. The oxygen-dependent type I mechanism can be outlined with a two-step reaction scheme.

dx.doi.org/10.1021/jp3068359 | J. Phys. Chem. B 2012, 116, 10816−10823

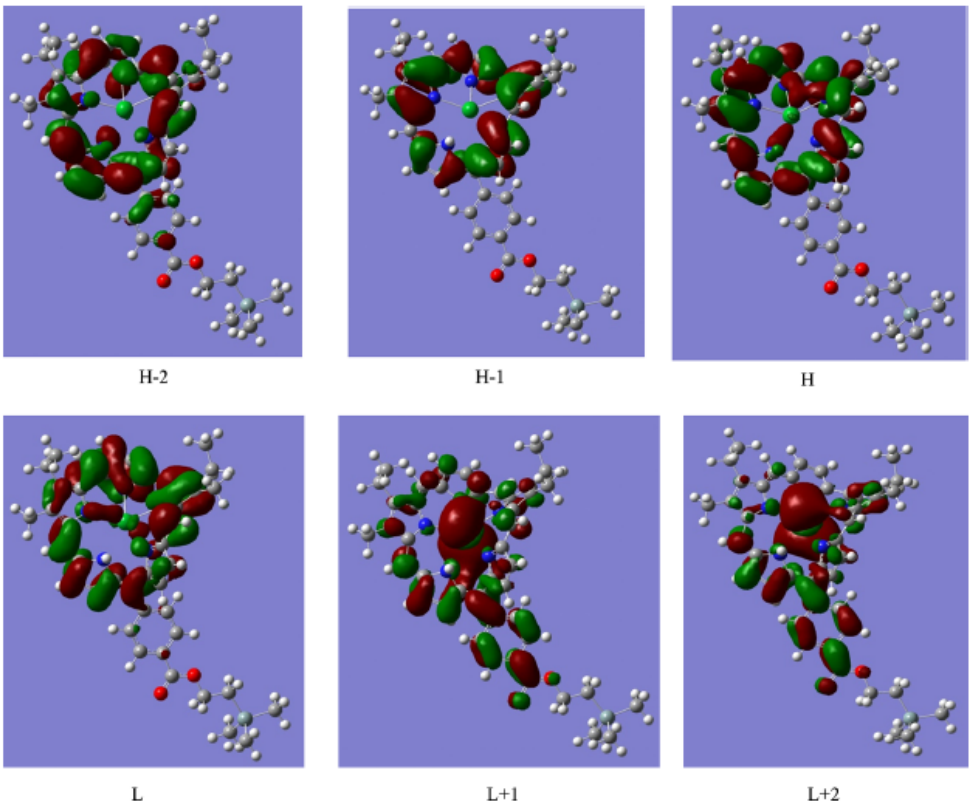

Figure 4. Frontier molecular surface plots (from HOMO $-n$ to LUMO $+n$) with isodensity value of 0.02 au, for compound **2** calculated at the ωB97X/SV(P)-SDD level of theory and solvent model.

Initially (step a), the photosensitizer, in its excited triplet state (^{3}Ps*), oxidizes the substrate:

$$^3\text{Ps}^* + \text{S} \rightarrow \text{Ps}^{\bullet(-)} + \text{S}^{\bullet(+)} \quad \text{(a)}$$

Then, the reduced photosensitizer form reacts with molecular dioxygen to give the superoxide radical ion $O_2^{\bullet(-)}$ (step b):

$$\text{Ps}^{\bullet(-)} + {}^3\text{O}_2 \rightarrow {}^1\text{Ps} + \text{O}_2^{\bullet(-)} \quad \text{(b)}$$

The superoxide ion is supposed to promote indirectly the generation of ROS species by reacting with biomolecules. An important thermodynamic factor determining the energetic process, which can be computed theoretically, is given by the electron affinities of the photosensitizer in the ground (VEA) and excited triplet states (VEA(T_1)). These two parameters should be compared with the ionization potential of the substrate (step a) and that of dioxygen (step b), in order to predict if the respective reactions are energetically favorable. The vertical electron affinities of **1** and **2** were computed *in vacuo* considering two different constants (dichloromethane and water) (see Table 4) at the PBE0 and B3LYP levels of theory, since the performance of these functionals in this field has been previously tested.[40,41] The VEA values range between 1.76 and 3.23 eV (PBE0) with an increasing value in aqueous medium due to the better charge stabilization of the photosensitizer anionic form. The corresponding vertical electron affinities in the excited triplet state lie nearly in the same range 1.86−3.34 eV (PBE0), due to the small contribution of the triplet energies (E_T). The B3LYP computed electron affinities differ by almost 0.1 eV. For the ground state dioxygen, the computed adiabatic electron affinity *in vacuo* is found to be 0.34 and 0.51 eV at the PBE0/def2-SVP and B3LYP levels, respectively. The experimental value is 0.45 eV.[42] The inclusion of bulk aqueous solvation effects gives a value of 3.84 eV (3.99 eV for B3LYP). Comparing the electron affinity of dioxygen in water with the corresponding values for **1** and **2**, and supposing that the reduced photosensitizer form was generated, the reaction in aqueous solution is predicted to be favorable with an energy gain of 0.5 eV.

3.3.2. Type II Reaction Mechanism. For this mechanism, the photocytotoxic activity is caused by the reactive singlet oxygen ($^1\Delta_g$), that is generated through the energy transfer process between the photosensitizer excited lowest triplet state (Ps(T_1)) and ground state dioxygen ($^3O_2$), as follows:

$$\text{Ps}(\text{T}_1) + {}^3\text{O}_2 \rightarrow \text{Ps}(\text{S}_0) + {}^1\text{O}_2$$

The generated singlet oxygen ($^1O_2$) exerts cytotoxic effects against the cellular environment with high selectivity due to its short lifetime (4 μs).[18] To be effective, this mechanism requires that the triplet energy of the photosensitizer should be at least equal to that of $^3O_2$. For the latter, the experimental value for the electronic transition $^3O_2(^3\Sigma_g^+) \rightarrow {}^1O_2(^1\Delta_g)$ is found to be 0.98 eV.[43] From Table 4, since the triplet energies (E_T) for the investigated molecules are by far lower that the above-stated energetic limit, we can conclude that at least theoretically they cannot generate singlet oxygen. The use of the 9,10-dimethylanthracene experimental test, by Comuzzi et al.,[20] has not detected the generation of singlet oxygen after irradiation of compounds **1** and **2**, confirming in this way the too low calculated triplet energies (<0.3 eV). This evidence rules out the

dx.doi.org/10.1021/jp3068359 | J. Phys. Chem. B 2012, 116, 10816−10823

Table 4. Triplet Energies (E_T), Ground State Vertical Electron Affinities (VEA), and Ionization Potentials (VIP) for 1 and 2 Molecules, Calculated at the def2-SVPD/PBE0//def-SV(P)/PBE0 Level (B3LYP in Parentheses)[a]

Compound 1													
E_T			VEA			VEA(T_1)[b]			VIP			VIP(T_1)[c]		
$\varepsilon = 0$	$\varepsilon_{CH_2Cl_2}$	ε_{H_2O}	$\varepsilon = 0$	$\varepsilon_{CH_2Cl_2}$	ε_{H_2O}	$\varepsilon = 0$	$\varepsilon_{CH_2Cl_2}$	ε_{H_2O}	$\varepsilon = 0$	$\varepsilon_{CH_2Cl_2}$	ε_{H_2O}	$\varepsilon = 0$	$\varepsilon_{CH_2Cl_2}$	ε_{H_2O}
0.13	0.11	0.11	1.78	3.00	3.23	1.91	3.11	3.34	5.25	4.36	4.21	5.12	4.25	4.10
(0.31)	(0.29)	(0.29)	(1.64)	(2.89)	(3.12)	(1.95)	(3.18)	(3.41)	(5.21)	(4.33)	(4.18)	(4.90)	(4.04)	(3.89)
Compound 2														
E_T			VEA			VEA(T_1)			VIP			VIP(T_1)		
$\varepsilon = 0$	$\varepsilon_{CH_2Cl_2}$	ε_{H_2O}	$\varepsilon = 0$	$\varepsilon_{CH_2Cl_2}$	ε_{H_2O}	$\varepsilon = 0$	$\varepsilon_{CH_2Cl_2}$	ε_{H_2O}	$\varepsilon = 0$	$\varepsilon_{CH_2Cl_2}$	ε_{H_2O}	$\varepsilon = 0$	$\varepsilon_{CH_2Cl_2}$	ε_{H_2O}
0.10	0.13	0.13	1.76	2.93	3.14	1.86	3.06	3.27	5.11	4.18	4.02	5.01	4.05	3.99
(0.12)	(0.13)	(0.13)	(1.69)	(2.96)	(3.04)	(1.81)	(3.09)	(3.17)	(5.02)	(4.07)	(3.90)	(4.90)	(3.94)	(3.77)
Dioxygen														
VEA						VIP								
$\varepsilon = 0$			$\varepsilon_{CH_2Cl_2}$			ε_{H_2O}			$\varepsilon = 0$			$\varepsilon_{CH_2Cl_2}$		ε_{H_2O}
0.34			3.34			3.84			12.6			9.44		8.91
(0.51)			(3.50)			(3.91)			(12.7)			(9.49)		(8.96)

[a]All the data, in *vacuum* and COSMO model, at different dielectric constants [ε_{H_2O} = 78.39 and $\varepsilon_{CH_2Cl_2}$ = 8.93], are reported in eV. [b]First triplet excited state electron affinities: VEA(T_1) = VEA + E_T. [c]First triplet excited state ionization potentials: VIP(T_1) = VIP − E_T.

type II mechanism as being the photochemical pathway for the high cytotoxic activity found for compound **2**.

3.3.3. Direct Electron Transfer to Dioxygen. The possible photo-oxidation of the photosensitizer, in the ground or excited state, by dioxygen, according to the following reaction

$$Ps(S_0/T_1) + {}^3O_2 \rightarrow Ps^{\bullet(+)} + O_2^{\bullet(-)}$$

can be another source for generating cytotoxic species (e.g., H_2O_2, $^{\bullet}OH$), after the bimolecular decay of the superoxide ion. This reaction mechanism is possible if the dioxygen is able to capture an electron from the photosensitizer, or in other terms the electron affinity of dioxygen is greater than the ionization potential of the photosensitizer. The vertical ionization potentials for **1** and **2**, for the ground (VIP) and lowest triplet excited state (VIP(T_1)), are reported in Table 4 for *in vacuo*, dichloromethane and water solution. The *in vacuo* PBE0 ionization potentials (VIP) are 5.25 and 5.11 eV for **1** and **2**, respectively (5.21 and 5.02 eV for B3LYP). The aqueous VIP values are smaller by about 0.1 eV. Considering that the electron affinity of O_2 in water, from both PBE0 and B3LYP calculations, is smaller than the studied molecules' VIPs, the reaction is not energetically feasible. However, for the lowest triplet excited state VIPs calculated at the B3LYP level, an energy gain in water solution of 0.1−0.2 eV is predicted. From Table 4, we observe that the higher ionization potential for dioxygen, *in vacuo* and water solution (>8.9 eV), in comparison with that of the pentaphyrin derivatives **1** and **2**, seems to prevent the possibility that O_2 could be oxidized by the photosensitizer.

3.3.4. Autoionization of Isopentaphyrin Derivatives. After being excited to the lowest triplet state, a photosensitizer molecule, $Ps(T_1)$, can be reduced by an identical molecule in its ground state (a) or triplet excited state (b) as follows:

$$Ps(T_1) + Ps(S_0) \rightarrow Ps^{\bullet(-)} + Ps^{\bullet(+)} \quad (a)$$

$$Ps(T_1) + Ps(T_1) \rightarrow Ps^{\bullet(-)} + Ps^{\bullet(+)} \quad (b)$$

For reaction a, the comparison between the PBE0 VEA values for the T_1 state (3.34 and 3.27 eV for **1** and **2**) and the ground state VIP ones (4.21 and 4.02 eV), computed in water, indicates that the process is endothermic and therefore not energetically favorable. This conclusion is still valid for the gas-phase and dichloromethane calculations. The autoionization process, considering both molecules lying at the first triplet excited states (reaction b), is also predicted unfavorable in the gas phase ($\varepsilon = 0$) and solutions ($\varepsilon = 8.93$ and $\varepsilon = 78.39$). The energy gain is negative (endothermic process) by more than 0.7 eV for both compounds **1** and **2** (see Table 4).

4. CONCLUDING REMARKS

The gas-phase optimized structures of the isopentaphyrin derivative **1** and its lutetium complex **2**, investigated in this work, display a high degree of distortion of the macrocycle, as can be seen from the dihedral angle value between the adjacent pyrrolic rings. This feature is basically due to the lack of electronic conjugation for these nonaromatic compounds. The main geometrical parameters derived from DFT calculations are almost similar for the exchange-correlation functionals employed for this purpose (PBE0, B3LYP, ωB97X, and ωB97XD). For the free metal isopentaphyrin, the lowest excitation energy or Q-band absorption is predicted at 772 nm with a low oscillator strength (in dicloromethane solution), by using the ωB97XD functional. The deviation error from the corresponding experimental absorption peak is about 0.1 eV. For the lutetium complex, an absorption peak in the Q-region is still predicted very weak, though it does not appear in the experimental spectrum. The triplet energies of these compounds are smaller than 0.3 eV, ruling out the ability to generate singlet oxygen by means of a type II PDT mechanism. Other mechanisms (type I mechanism and direct electron transfer to O_2), which can form reactive and cytotoxic oxygen species, have been analyzed by computing the energy gain for the model reaction. In particular, considering the energetic parameters involved in the type I mechanism (electron affinities and ionization potentials), the reaction is predicted energetically possible (exothermic process), in a solution simulating the water dielectric constant.

dx.doi.org/10.1021/jp3068359 | J. Phys. Chem. B 2012, 116, 10816−10823

■ ASSOCIATED CONTENT

Supporting Information

In vacuo optimized Cartesian coordinates for compounds **1** and **2** calculated at the PBE0/SV(P) level. This material is available free of charge via the Internet at http://pubs.acs.org.

■ AUTHOR INFORMATION

Corresponding Author

*Phone: +39-0984-492048. Fax: +39-0984-492044. E-mail: nrusso@unical.it.

Notes

The authors declare no competing financial interest.

■ ACKNOWLEDGMENTS

Financial support from the Università degli Studi della Calabria and MIUR (PRIN 2008) is gratefully acknowledged.

■ REFERENCES

(1) Dolphyn, D. *The Porphyrins*; Academic Press: New York, 1978; Vol. *I*.
(2) Falk, J. E. *Porphyrins and Metalloporphyrins*; Elsevier: Amsterdam, The Netherlands, 1964.
(3) Gouterman, M. *J. Mol. Spectrosc.* **1961**, *6*, 138−163.
(4) Saito, S.; Osuka, S. A. *Angew. Chem., Int. Ed.* **2011**, *50*, 4342−4373.
(5) Jasat, A.; Dolphin, D. *Chem. Rev.* **1997**, *97*, 2267−2340.
(6) Woodward, R. B. *Aromaticity: An International Symposium*, Sheffield, U.K., 6-9 July, 1966; Special publication no. 21; The Royal Chemical Society: London, U.K., 1966.
(7) Bauer, V. J.; Clive, D. L. J.; Dolphyn, D.; Paine, J. B.; Harris, F. L.; King, M. M.; Loder, J.; Wang, S. W. C.; Woodward, R. B. *J. Am. Chem. Soc.* **1983**, *105*, 6429−6436.
(8) Sessler, J. L.; Seidel, D. *Angew. Chem., Int. Ed. Engl.* **2003**, *42*, 5134−5175.
(9) Franck, B.; Nonn, A. *Angew. Chem., Int. Ed. Engl.* **1995**, *34*, 1795−1811.
(10) Sessler, J. L.; Hemmi, G.; Mody, T. D.; Murai, T.; Burrell, A.; Young, S. W. *Acc. Chem. Res.* **1994**, *27*, 43−50.
(11) Young, S. W.; Qing, F.; Harriman, A.; Sessler, J. L.; Dow, W. C.; Mody, T. D.; Hemmi, G. W.; Hao, Y.; Miller, R. A. *Proc. Natl. Acad. Sci. U.S.A.* **1996**, *93*, 6610−6615.
(12) Ahn, T. K.; Kwon, J. H.; Kim, D. Y.; Cho, D. W.; Jeong, D. H.; Kim, S. K.; Suzuki, M.; Shimizu, S.; Osuka, A.; Kim, D. *J. Am. Chem. Soc.* **2005**, *127*, 12856−12861.
(13) Sessler, J. L.; Cyr, M.; Furuta, H.; Král, V.; Mody, T.; Morishima, T.; Shionoya, M.; Weghorn, S. *Pure Appl. Chem.* **1993**, *65*, 393−398.
(14) Burrell, A. K.; Hemmi, G.; Lynch, V.; Sessler, J. L. *J. Am. Chem. Soc.* **1991**, *113*, 4690−4692.
(15) Sessler, J. L.; Tomat, E. *Acc. Chem. Res.* **2007**, *40*, 371−379.
(16) Bonnett, R. *Chemical Aspects of Photodynamic Therapy*; Gordon & Breach Science Publishers: Amsterdam, The Netherlands, 2000.
(17) O' Connor, A. E.; Gallagher, W. M.; Byrne, A. *Photochem. Photobiol.* **2009**, *85*, 1053−1074.
(18) Ogilby, P. *Chem. Soc. Rev.* **2010**, *39*, 3181−3209.
(19) Turro, N. J. *Modern Molecular Photochemistry*; Benjamin: Menlo Park, CA, 1978.
(20) Ballico, M.; Rapozzi, V.; Xodo, L. E.; Comuzzi, C. *Eur. J. Med. Chem.* **2011**, *46*, 712−720.
(21) Becke, A. D. *J. Chem. Phys.* **1993**, *98*, 5648−5652.
(22) Adamo, C.; Barone, V. *J. Chem. Phys.* **1999**, *110*, 6158−6170.
(23) Ernzerhof, M.; Scuseria, G. E. *J. Chem. Phys.* **1999**, *110*, 5029−5036.
(24) Chai, J. D.; Head-Gordon, M. *J. Chem. Phys.* **2008**, *128*, 84106−84155.
(25) Chai, J. D.; Head-Gordon, M. *Phys. Chem. Chem. Phys.* **2008**, *10*, 6615−6620.
(26) Jacquemin, D.; E. Perpete, E. A.; Ciofini, I.; Adamo, C. *Acc. Chem. Res.* **2009**, *42*, 326−334.
(27) Send, R.; Kühn, M.; Furche, F. *J. Chem. Theory Comput.* **2011**, *7*, 2376−2386.
(28) Schäfer, A.; Horn, H.; Ahlrichs, R. *J. Chem. Phys.* **1992**, *97*, 2571−2577.
(29) Cao, C. X.; Li, Q.; Moritz, A.; Xie, Z.; Dolg, M.; Chen, X.; Fang, W. *Inorg. Chem.* **2006**, *45*, 3444−3451.
(30) Casida, M. E. In *Recent Developments and Applications in Density-Functional Theory*; Seminario, J. M., Eds.; Elsevier: Amsterdam, The Netherlands, 1996; pp 155−192.
(31) Tian, B.; Eriksson, E. S. E.; Eriksson, L. A. *J. Chem. Theory Comput.* **2010**, *6*, 2086−2094.
(32) Eriksson, E. S. E.; Eriksson, L. A. *Phys. Chem. Chem. Phys.* **2011**, *13*, 7207−7217.
(33) Klamt, A.; Schüürmann, G. *J. Chem. Soc., Perkin Trans. 2* **1993**, *5*, 799−805.
(34) Rappoport, D.; Furche, F. *J. Chem. Phys.* **2010**, *133*, 134105−134111.
(35) Ahlrichs, R.; Bär, M.; Häser, M.; Horn, M.; Kölmel, C. *Chem. Phys. Lett.* **1989**, *162*, 165−169.
(36) Frisch, M. J.; Trucks, G. W.; Schlegel, H. B.; Scuseria, G. E.; Robb, M. A.; Cheeseman, J. R.; Montgomery, J. A., Jr.; Vreven, T.; Kudin, K. N.; Burant, J. C.; et al. *Gaussian 03*, revision C.02; Gaussian, Inc.: Wallingford, CT, 2004.
(37) Gouterman, M.; Wagnière, G. H.; Snyder, L. C. *J. Mol. Spectrosc.* **1963**, *11*, 108−127.
(38) Shin, J-Y; Kim, K. S.; Yoon, M-C; Lim, J. M.; Yoon, Z. S; Osuka, A.; Kim, D. *Chem. Soc. Rev.* **2010**, *39*, 2751−2767.
(39) Yoon, M-C; Cho, S.; Suzuki, M; Osuka, A.; Kim, D. *J. Am. Chem. Soc.* **2009**, *131*, 7360−7367.
(40) Guedes, R. C.; Eriksson, L. A. *Photochem. Photobiol. Sci.* **2007**, *6*, 1089−1096.
(41) Quartarolo, A. D.; Chiodo, S. G.; Russo, N. *J. Comput. Chem.* **2011**, *33*, 1091−1100.
(42) Travers, M. J.; Cowles, D. C.; Ellison, G. B. *Chem. Phys. Lett.* **1989**, *164*, 449−455.
(43) Herzberg, G. *Spectra of Diatomic Molecules*, 2nd ed.; Van Nostrand Reinhold: New York, 1950.

5) Squarines

Although some drugs based on the porphyrin are already approved and being used in hospitals (fig. 1), the research in this field continues actively with the goal in finding new drugs. This is because porphyrin based drugs have some disadvantages, namely they don't absorb efficiently on the therapeutic window due to low molar coefficients and possess side effects like cutaneous photosensitivity and immunosuppression. Many other molecules are under study (fig. 2) [1]

One of the new promising drugs are the squarines.

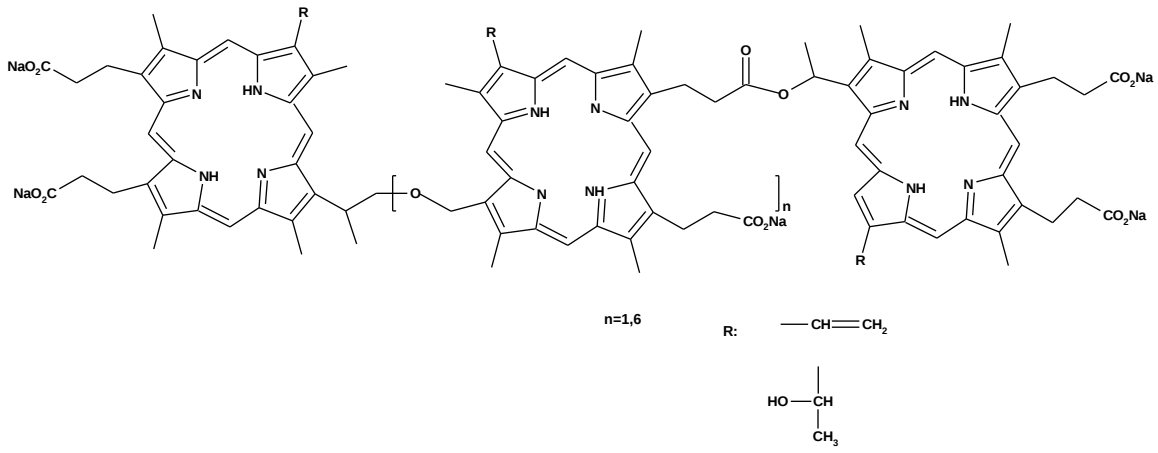

Figure 1

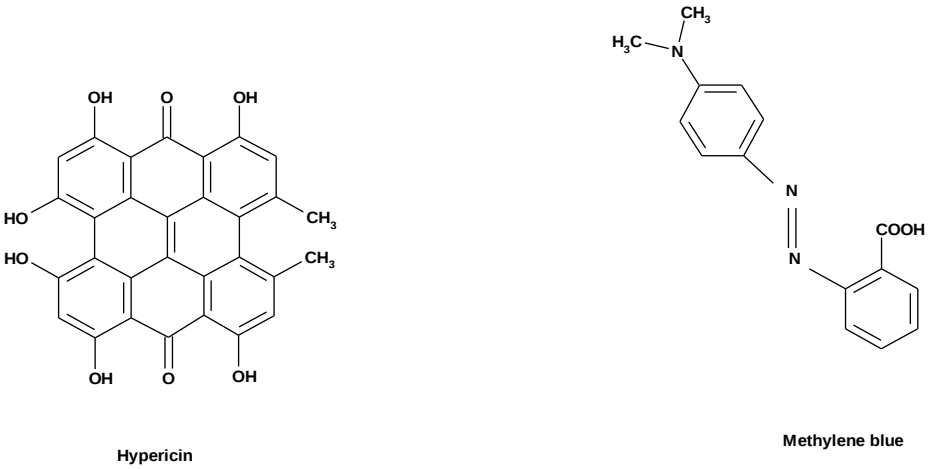

Figure 2

Squarines

Squarines are a class of organic compounds derived from the condensation reaction between squaric acid and an electron-rich compound [2].

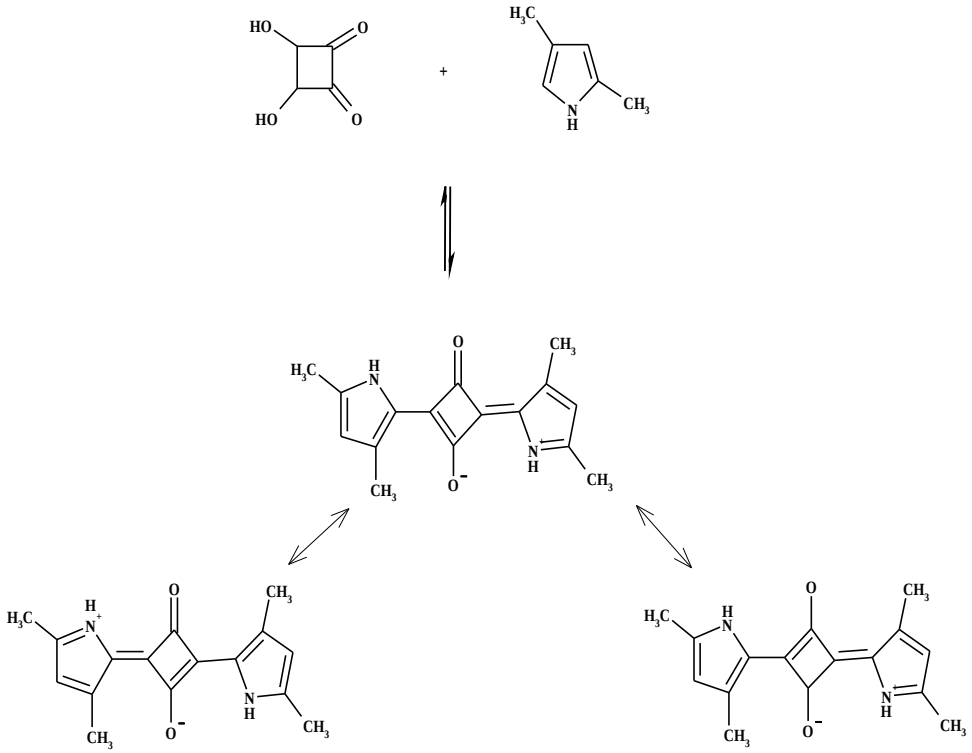

Figure 3

On figure 3 we show the resonance structures of the squarine deriving from the condensation of 2,4-dimethylpyrrole and squaric acid, one of the simplest derivatives described. Formally the core part of these compounds can be described by three resonance structures with 12 π-electrons and a positive charge delocalized through the two symmetrical moieties. These compounds are characterized by a sharp intense absorption band ($\varepsilon \sim 10^5\ M^{-1}cm^{-1}$) between 500-800 nm, where tissues are fairly transparent to light. Their absorption and photochemical characteristics make them highly suitable for a number of industrial applications such as dye- sensitized solar cells, optical storage devices, fluorescence probes for detecting metal ions and in photosensitizer drug in Photodynamic Therapy.

Early work on squarines has been focused on solar energy conversion. Recently, Yum J-H et al [3] al

reported on the synthesis of a new asymmetric squarine (636 nm, $\varepsilon = 1.5\times10^{5}\ M^{-1}\ cm^{-1}$) that has a carboxylic acid group directly attached to the chromophore (figure 4). It was observed that the inclusion of these squarines on solar cells gave high photocurrent and overall photovoltaic efficiency for the solar cell what was directly related with the high absorption of this molecule.

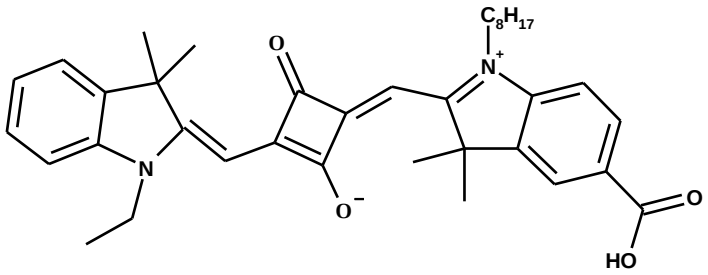

Figure 4

The potential of squarine's use on PDT is been being studied on the last times.

The work of Ramaiah et al [4] reported the synthesis of a new class of halogenated squarines (fig. 5) designed for PDT sensitizers.

The inclusion of heavy elements, bromine in Sq_2 and Iodine in Sq_3 would increase the intersystem crossing and, in consequence, the production of triplet state while the molecule hydroxide groups guarantee the solubility in the aqueous solutions.

Depending on the pH of the solution, it was shown that each compound could be in four protonation state - protonated SqH^{+}, neutral Sq, single deprotonated Sq^{-} and doubly deprotonated $Sq^{2,-}$, being that at cellular pH the single deprotonated form Sq^{-} is predominat form. The apparent form of the deprotonated form Sq^{-} has a wavelength absorption at 610 nm, and the halogention change is to 617 nm for the case of bromine derivative and to 588 nm for the case of iodine, for which we conclude that the inclusion of the heavy elements maintain the absorption on the therapeutic window.

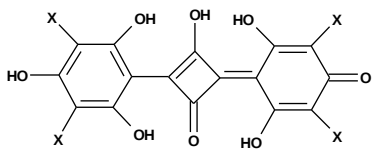

1) X=H
2) X=Br
3) X=I
3)

Figure 5

To analyze the effect of the medium, the absorption of Sq^- on the presence of solubilization agents $_\beta$CD, CTAB and PVP were studied. CTAB forms micelles above its critical micellar concentration that confers it a hydrophobic character on the inner region and hydrophilic on the outer region whereas PVP forms a micro cage, which is hydrophobic in nature. The single deprotonated forms of the bromide and iodine derivatives showed a red shift on the range 8-34 nm indicating a stabilization of this protonation form and, since it is predominant specie under the biological pH condition, the authors suggested that these solubilization agents could be explored as drug delivery systems.

The triplet lifetimes were investigated where it was concluded that the triplet states of 2 and 3 are long lived and that the Sq^- form has the higher lifetime followed by the neutral form.

The triplet quantum yield Φ_T, a very important factor that reflects the efficiency of the intersystem crossing from the singlet state to the triplet state, was studied. The Sq^- showed accentuated production of triplet state, a Φ_T of 0.5 for iodine a value much higher than the 0.22 found for bromine 0.22. This result is in agreement with the theory that states that the intersystem crossing efficiency increases with the atomic number.

The crucial variable is the singlet oxygen quantum yield which measures the production of the sinlget oxygen and it depends on the parameters of all the processes that take place until the singlet oxygen is formed. The study concerned the single deprotonated form where the iodine derivative showed a higher value Φ_T of 0.47 in comparison of the 0.13 obtained with the bromine derivative.

The other work of Ramaiah et all [5] studied the toxicity of these compounds on mammalian and bacterial cells. The results showed that on the presence of radiation the halogenated squarines exhibit efficient cytotoxicity while in the dark the toxicity of these compounds were much less toxic. The iodine derivative showed greater toxicity that the bromide one. This fact suggested the occurrence of type I mechanism where the greater toxicity of this derivative is explained by its greater triplet state production. However, the authors considered that other mechanisms must have occurred because the difference in toxicity observed was much less than expected. They suggested that homolysis upon excitation occurs:

$$^3SqX \rightarrow Sq^{\bullet} + X^{\bullet}$$

$$^3SqX^- \rightarrow Sq^{\bullet} + X^{\bullet -}$$

what will form radicals form that will spread causing stress to the cell.

The works of Bonnett et al [6] and Beverina et al [7] reported on the synthesis and photo physical characterization of a new class of squarines containing an elongated π conjugation systems (figure 6) with three classes of molecules, from Domenico paper) designed to have a red-shifted absorption.

Table 1 showed the experimental values of maximum absorption λ_{max} for these compounds obtained as well as the TDDFT values calculated by Quartarolo et al. [8] We notice that the experimental λ_{max} falls on the range 623-728 nm, on the therapeutic window, while for TTDFT it falls on the 531-612 nm wavelengths with a mean absolute deviation of 0.31eV.

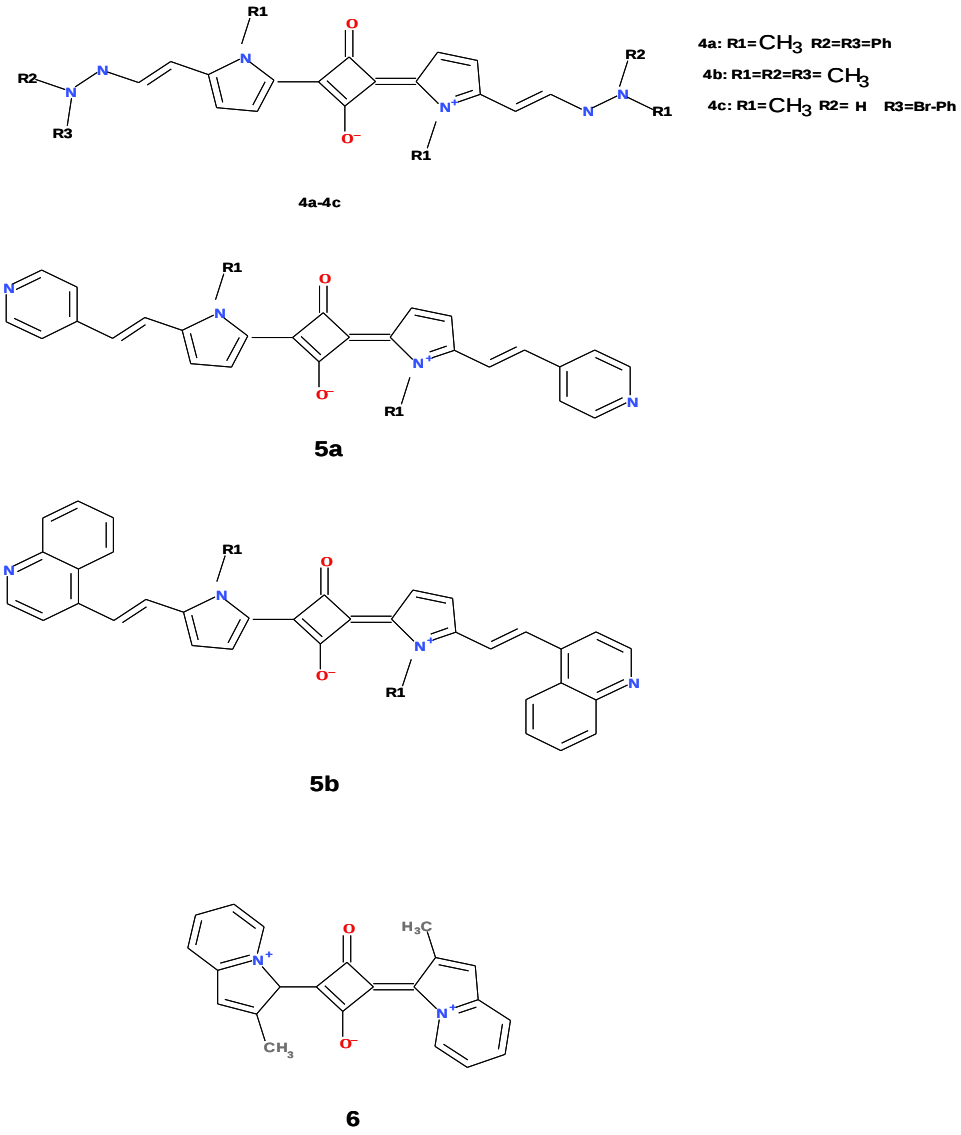

Figure 6

Table 1. TDDFT Singlet Excitation energies ΔE (eV and nm (in parentheses)) and Oscillator strenght by TDDFT calculated at PBE0/SVP level of theory

	1a	**1b**	**1c**	**1d**	**1e**	**2**	**3a**	**3b**	**4a**	**4b**	**4c**	**5a**	**5b**	**6**	**MAE**
ΔE	2.73	2.33	2.33	2.26	2.27	2.12	2.28	2.25	2.04	2.24	2.09	2.07	2.03	2.22	0.31
	(454)	(533)	(531)	(549)	(546)	(586)	(544)	(552)	(609)	(553)	(593)	(600)	(612)	(559)	
f	0.832	1.578	1.661	1.835	1.701	2.368	1.849	1.746	2.619	2.029	2.337	2.356	2.356	2.376	
exptl	----	2.00	1.98	1.93	2.02	1.84	1.90	1.88	1.70	1.80	1.73	1.83	1.80	1.81	
	----	(621)	(625)	(643)	(613)	(673)	(654)	(660)	(728)	(688)	(717)	(678)	(688)	(684)	

MAE is the mean absolute deviation

The work of Beverina et al also studied the production of singlet oxygen by monitoring the time disappearance of the absorption band at 415 nm of 1,3-diphenylisobenzofuran (DPBF). DPBF is known to form an endoperoxide upon cycloaddition with singlet oxygen, resulting in the complete disappearance of it's characteristic absorption band at 415 nm. The experimental results proved that the above mentioned compounds and in particular 4a and 4c (containing bromine atoms) are able to give a singlet oxygen yield.

Triplet energies calculated by Quartarolo et al are shown on table 2, in which we conclude that all the studied compounds have triplet energies below the limit of 0.98 eV. In particular, in vacuum, triplet energies are in the range between 0.61 (5b) and 0.95 eV (1a). Bulk salvation effects slightly increase the triplet excitation energies by 0.02-0.08 eV. It can be argued, from TDDFT, that only 1a-e, 3a-b, and 6 compounds lie close to the mentioned energetic gap.

Table 2. TDDDFT Triplet Energies (eV) in vacuo and with C-PCM at at the PBE0/SV(P) level of theory

	vacuo	c-pcm
1a	0.95	1.00
1b	0.85	0.88
1c	0.86	0.89
1d	0.85	0.87
1e	0.86	0.90
2	0.69	0.72
3a	0.87	0.90
3b	0.84	0.88
4a	0.65	0.72
4b	0.69	0.72
4c	0.65	0.71
5a	0.58	0.66
5b	0.61	0.69
6	0.91	0.96

Present work on squarines

In this work we focus on photophysical characterization on three recently synthetized taylored squarines [9,10], (figure 7). The 1a and 1b compounds are isomers and compound 2 has a substitution of the sulfur atom by a $C(CH_3)_2$ group.

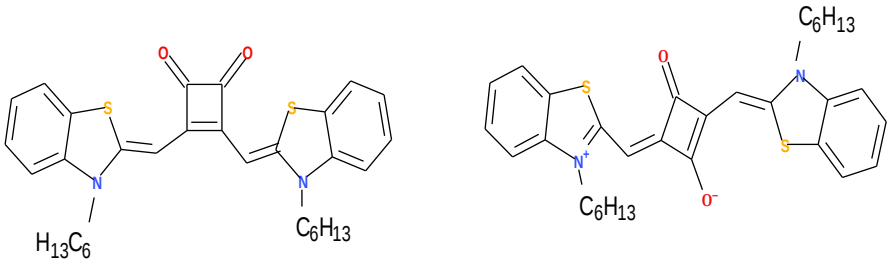

1a 1b

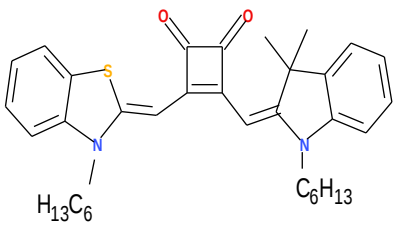

2

Figure 7

These squarines are designed to act on biological membranes causing lipid peroxidation and this is why they are prepared to have a hydrophobic hydrocarbon chain that allows solubility in the lipid phase. On figure 8 we show the optimized structures at DFT/PBE0/SV/(P) level of theory.

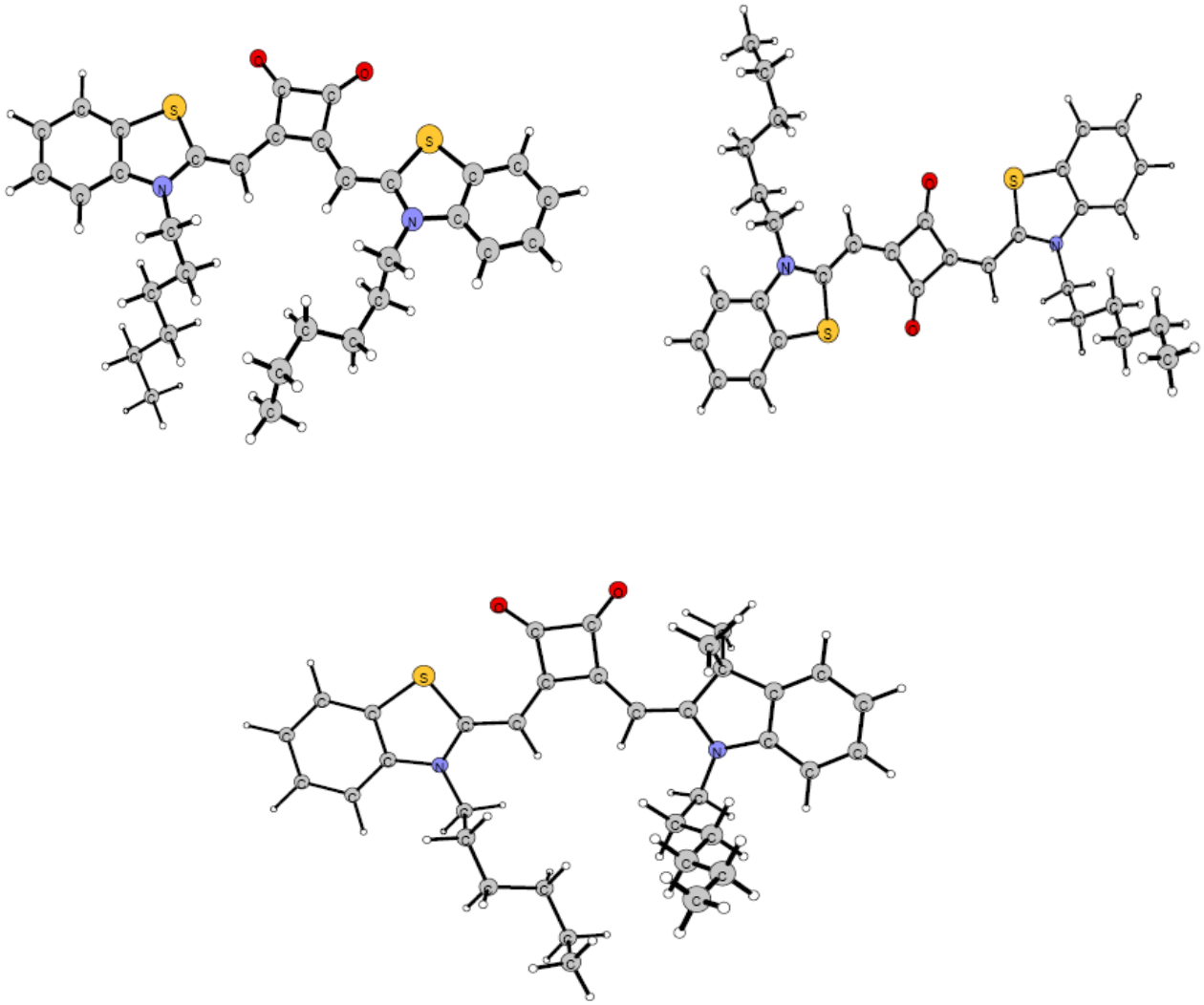

Figure 8

Experimental data shows that the absorption of compound 1b is more red shifted with the value of 659 nm while the 1a and 2 wavelengths are at 515 and 504 nm.

We started by investigating the basis set influences on λ_{max} for compound 1a, the results are reported in Table 3 and are relative to PBE0 calculations. It is evident that the increasing size of the basis set improves little on the agreement with the experimental λ_{max} (515 nm). So, a good compromise between computational timings and numerical reproduction of λ_{max} can be obtained by just employing a SVP basis.

The results for maximum absorption wavelength (λ_{max}) on toluene are shown on table 4. For 1a which the experimental λ_{max} on toluene was 515, nm we found that B3LYP functional gave the best

Table 3. Basis Set Influence for the First Excitation Energy ΔE (eV, nm) and Oscillator Strength f of Compound 6 on gas phase from TDDFT calculations

	TDDDFT			exptl	
Basis set	ΔE(eV)	ΔE (nm)	f	ΔE(eV)	ΔE (nm)
SV(P)	2.876	430.7	1.3979	2.40	515
SVP	2.875	431.1	1.3952		
DZP	2.871	431.7	1.3850		
TZVP	2.850	434.9	1.3531		
TZVPP	2.853	434.4	1.3334		
cc-pVDZ	2.877	430.8	1.3673		
cc-pVTZ	2.857	433.8	1.3343		
aug-cc-pVDZ	2.845	435.6	1.3262		

Table 4. First Excitation Energy((nm), gas phase in parentheses) and Oscillator Force calculated at TDDFT/DFT/SV(P)[a] level of theory, experimental Maximum Absorption Band(nm) (Molar Extinction Coefficient, ε (× 10^4 L $mol^{-1}cm^{-1}$) in parentheses) in toluene

		Theoretical			Exptl
		λ_{max}	f	configuration	λ_{max}
1a	PBE0	446 (430)	1.5308	H→L (98.7)	515 (6.91)
	B3LYP	460 (443)	1.4657	H→ L (98.5)	
	wB97X	408 (381)	1.8234	H→ L (93.2)	
	wB97XD	426 (398)	1.7497	H→L (95.3)	
1b	PBE0	583 (567)	1.5560	H→L (98.6)	659 (8.830)
	B3LYP	596 (581)	1.5154	H →L (98.6)	
	wB97X	616 (566)	1.6230	H→L(96.0)	
	wB97XD	613 (566)	1.6110	H→L (97.0)	
2	PBE0	442 (427)	1.4030	H →L(98.6)	504 (9.433)
	B3LYP	456 (440)	1.3341	H →L(98.5)	
	wB97X	402 (377)	1.7165	H→ L (92.4)	
	wB97XD	419 (393)	1.6230	H→ L (94.6)	

value, 460 nm, followed by PBE0 which gave 446 nm. With functional ωB97XD and ωB97X we obtained too much blue shifted values at 468 and 408 nm, respectively.

Also, table 3 shows that the absorption for B3LYP and PBE0 on gas phase come blue shifted, in relation to the solvent spectrum, by 17 and 16 nm respectively while for the functional ωB97X and

ωB97XD the blue shift also occurs but by more accentuated values of 27 and 28 nm, respectively, in relation the solvent spectrum

For the isomer 1b, the experimental λ_{max} is 659 nm. We found that the functional performance profile changed. The functional ωB97X gave the best value, 616 nm, followed by ωB97XD which gave 613 nm. The functionals B3LYP and PBE0 showed the poorest performance giving the values 596 and 583 nm, respectively. For the functional B3LYP and PBEO λ_{max} calculated at gas phase come blue shifted in relation to the solvent case by the same shift of squarine 1a. However, for ωB97X and ωB97XD these blue shifts take accentuated values of 50 and 47 nm, respectively.

We notice that the functional performance on squarine 2 takes the same profile as it took for squarine 1a. The experimental λ_{max} was at 504 nm and B3LYP functional gave the best value of 456 nm, followed by PBE0 which give 442 nm and ωB97X and ωB97XD gave 402 and 419 nm, respectively.

The calculation on gas phase showed that the situation is similar to the squarine 1a. In relation to the solvent, B3LYP and PBE0 gave blue shifts of 15 and 16 nm respectively while ωB97X and ωB97XD gave blue shifts of 25 and 26 nm respectively, less accentuated than for the squarine 1a case.

The conclusions for compound 1a applies to compound 2, suggesting that what really makes difference on the functional performance for the molecules studied could be on the molecular conformation rather than the substitution of the sulfur atom, since these two squarines share the same conformation.

On table 5 we show the triplet energies (E_T) (relative to the ground state) of the squarines calculated with three different approaches. By TDDFT, an approach that directly calculate the excitation energy - the increase in energy from the optimized ground state (gs) to the triplet energy frozen at the gs geometry, by vertical DFT vertical where we separately calculate the energy of the optimized gs and then the triplet at the frozen gs geometry and after takes the difference, and by adiabatic DFT where we optimize both states by DFT and take the difference.

We see that for squarines 1a and 2 the triplet energy is greater than the 0.98 eV necessary to excite oxygen to singlet state. For squarine 1b the TDDFT triplet energy is slightly below of what is necessary while the Adiabatic DFT (also vertical DFT) triplet energies is slightly above the limit of 0.98 eV.

This gives the question on which approach should we take. On table 6 we show E_T calculated with these three approaches versus the experimental E_T [8,11.]. We see that for benzene, the TDDFT result is

closer to the experimental E_T while for the other four molecules, naphthalene, antracene, pyrene and porphyrin the adiabatic DFT gives the results closer to the experiments.

Table 5. Triplet energies (eV) for the squarines on toluene (gas phase on parentheses), calculated at the PBE0/SV(P) level of theory.

	TD/DFT	DFT Vertical	DFT Adiabatic
1a	1.7278	1.8940	1.6849
	(1.7109)	(1.9960)	(1.6943)
1b	0.9118	1.0632	1.0094
	(0.8269)	(1.008)	(0.9521)
2	1.7428	1.9182	1.7003
	(1.7280)	(1.9207)	(1.7102)

Table 6. Gas Phase Triplet energies (eV) , calculated at the PBE0/SV(P) level of theory and experimental

	TD/DFT	DFT Vertical	DFT Adiabatic	Exptl.
Benzene	3.61	4.35	3.81	3.69
Naftalene	2.58	3.13	2.69	2.65
Antracene	1.64	2.10	1.77	1.82
Pyrene	1.98	2.42	2.07	2.08
Porphyrin	1.31	1.66	1.47	1.58

Bibliography

[1] Connor AEO, Gallagher WM and Byrne AT (2009)
Porphyrin and Nonporphyrin Photosensitizers in Oncology: Preclinical and Clinical Advances in Photodynamic Therapy
Vol 85, Issue 5, 1053-1074

[2] Law KY (1993)
Organic Photoconductive Materials: Recent Trends and Developments
Chemical Reviews Vol 93, Issue 1, 449-486

[3]Yum JH, Walter P, Huber S et al (2007)
Efficient Far Red Sensitization of Nanocrystalline TiO_2 Films by an Unsymmetrical Squaraine Dye
Journal of the American Chemical Society, Vol 129, Issue 34, 10320

[4] Ramaiah D, Joy A, Chandrasekhar N et al. (1997)
Halogenated Squaraine Dyes as Potential Photochemotherapeutic Agents. Synthesis and Study of Photophysical Properties and Quantum Efficiencies of Singlet Oxygen Generation
Photochemistry and Photobiology, Vol 65, Issue 5, 793-790

[5] Ramaiah D, Eckert I, Arun KT et al (2002)
Squaraine dyes for photodynamic therapy: Study of their cytotoxicity and genotoxicity in bacteria and mammalian cells
Photochemistry and Photobiology, Vol 76, Issue 6, 672-677

[6] Bonnett R, Motevalli M, Siu J (2004)
Squaraines based on 2-arylpyrroles, TETRAHEDRON Vol 60, Issue 40, 8913-8918

[7] Beverina L, Abbotto A, Landenna M, Cerminara M, Tubino R, F, Bradamante S, A. Pagani GA. (2011)
New π-Extended Water-Soluble Squaraines as Singlet Oxygen Generators
Organic Letters, Vol 7 Issue 19, 4257-4260

6) Corroles

Corroles are analogues of porphyrins with the specificity that two of the pyrrol rings are directly connected instead of being connected by a methine bridge (=CH-) (figure 1).

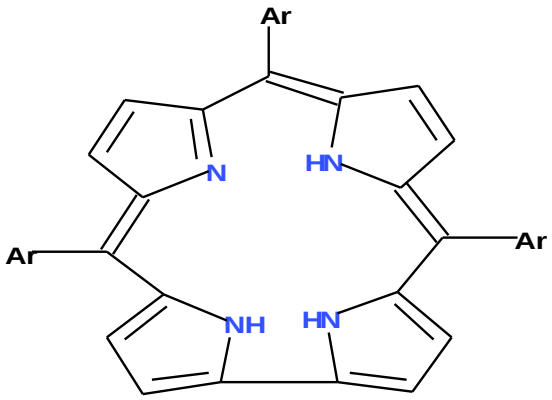

FIGURE 1

Like porphyrin they are aromatic macrocycles with an inner cavity containing four nitrogen atoms as an equatorial coordination template for metal ions. The corroles coordination plane is triprotonic and somewhat contracted what give to them some remarkable effects on the coordination chemistry, among which the stabilization of exceptionally high metal oxidation states is most outstanding. Further, the macrocycle is less symmetric compared to porphyrins and, in consequence, is that while substitution of one of the inner NH protons in porphyrins leads to a single product, two isomers are formed in the case of corroles (figure 2).

The most studied corroles appear to be tpfc and tphfcorroles (figure 3) [1,2] and its gallium complex. Its metal complexes are excellent catalysts for organic reaction, a water soluble derivative has a large affinity to cancer cells, chiral derivatives are easily prepared and many of its metal complexes have been characterized by X-ray crystallography.

The presence of β-pyrrole CH's in meso-arylcorroles opens up the opportunity for relatively straightforward skeleton modification. On a work by Mahammed et al [3] it was shown that the functionalization of corroles can be used for the easy preparation of amphiphilic derivatives with a metal ion (figure 4).

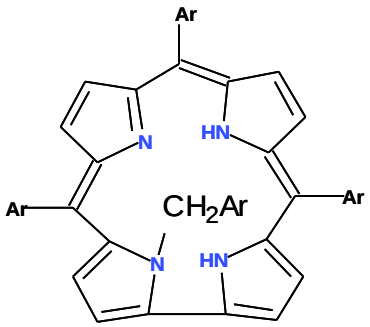

isomer 1

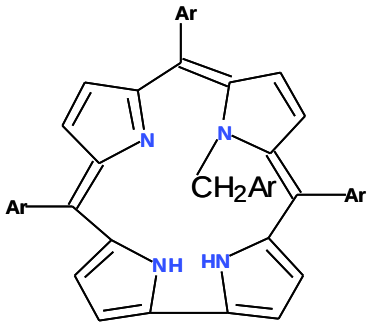

isomer 2

Figure 2

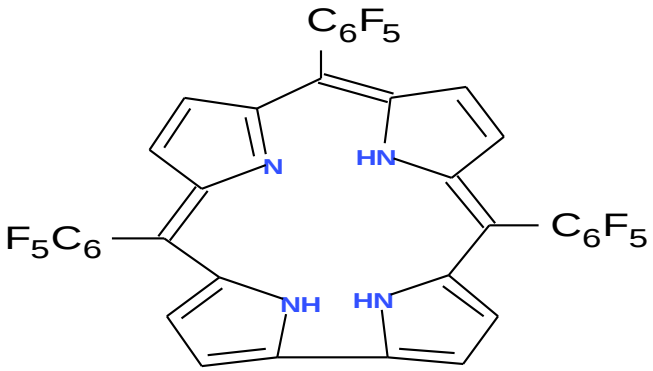

Figure 3

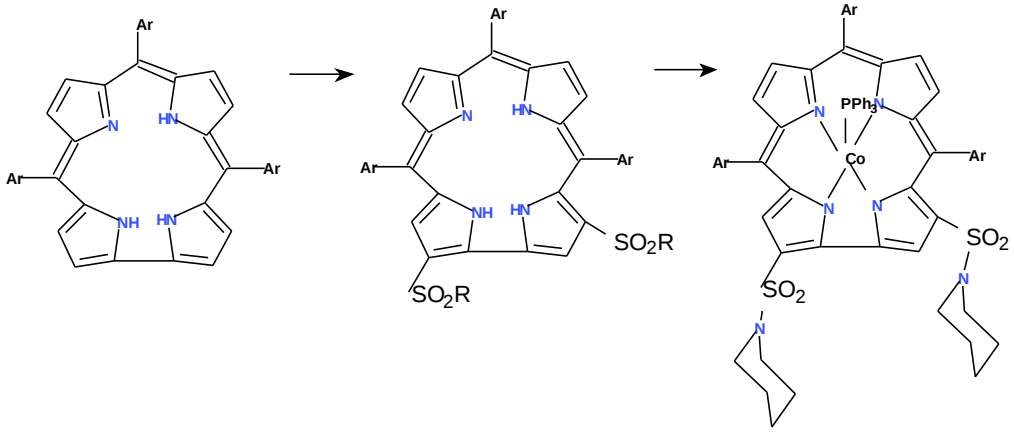

Figure 4

Recently, by a work on the group of Gross[4], was reported the synthesis of two new modified corroles, 1-Al and 4-Al. (figure 5), designed to be used on PDT. These compounds contains an aluminum ion on the cavity and on the periphery four iodine atoms. The metal of choice was aluminum(III) because its complexes have the highest emission quantum yields on record while the iodine atoms were incorporated with the aim to increase the intersystem crossing.

Importantly for PDT was the finding that the compound 4-Al produces a long-lived triplet state upon electronic excitation of the complex, with lifetimes 92 and 1 μs in degassed and aerobic toluene, respectively, what makes it is useful on PDT.

The compounds retains a planar macrocyclic framework, with the aluminum hexa coordinated - with four nitrogens of the macrocycle and with two pyridine molecules perpendicular to the plane.

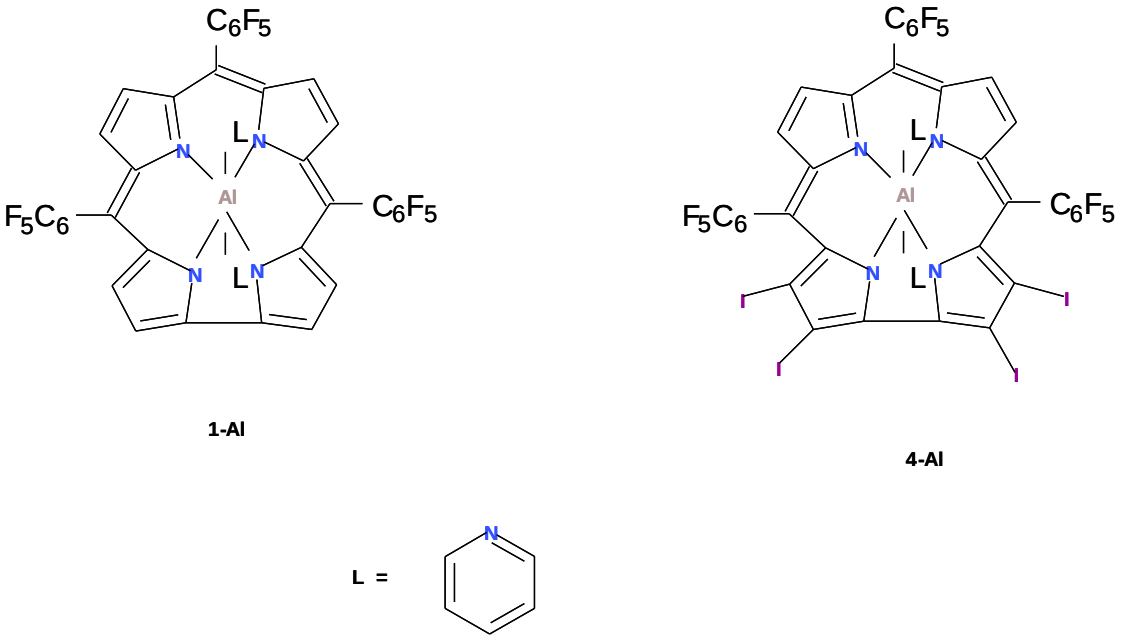

Figure 5

On figure 6 we show the optimized structures of these two compounds. Table 1 shows that the presence of iodides increases the Al-N(pyrrole) bond lengths by 0.002 – 0.016 while it decreases the Al-N(pyridine) distances. This bond shortening is consistent with the expected electronic e**ff**ect of the iodides: the Lewis acidity of the aluminum center is enhanced by removal of electron density from the pyrrole nitrogen atoms. This finding is consistent with experimental facts that shows that the equilibrium constant for the equilibrium involving the mono and bispyridine-coordinated forms of 4-Al is 508 M^{-1} which is nearly 4 times larger than that of 1-Al (135 M^{-1}).

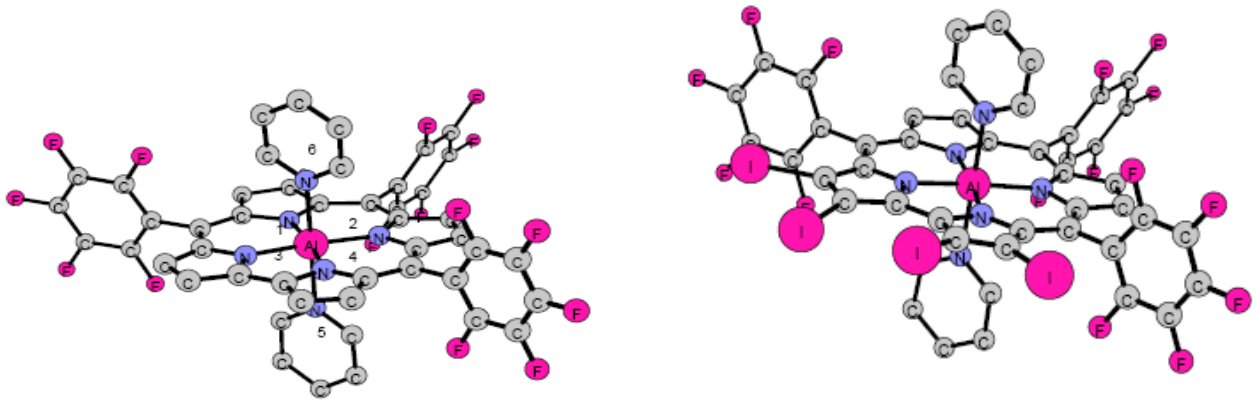

Figure 6

Table 1. Selected Geometrical parameters (nm) at DFT/PBE0/SV(P) level of theory experimental values in parentheses

	1 Al	4 Al
Al-N_1	1.90781 (1.8873)	1.91035 (1.89192)
Al-N_2	1.90897 (1.8998)	1.91092 (1.88209)
Al-N_3	1.90694 (1.8907)	1.92283 (1.91233)
Al-N_4	1.90606 (1.8947)	1.92231 (1.91051)
Al-N_5	2.20277 (2.2152)	2.19084 (2.17322)
Al-N_6	2.20436 (2.2011)	2.19442 (2.17876)

The experimental UV-vis spectra of both compounds have a very intense absorption on the Soret bands, 432 and 446 nm for 1-Al and 4-Al respectively, and two less intense peaks at Q-band, 582, 620 nm for 1-Al and 604, 637 nm for 4-Al (figure 7).

On table 2 we report the $\lambda_{max,}$, for the two compounds and also for Gallium, Iridium complexes and for the free bases (fb), from where we conclude that the incorporation of iodine red shifts the λ_{max} for all of the metals including the free base. We see that the metal insertion red-shifts the λ_{max} in relation to the free base with exception of the iridium complex that keeps the value for the case 1 (1 fb vs 1 Ir) and blue-shitfts the value for case 4 (4 fb vs 4 Ir).

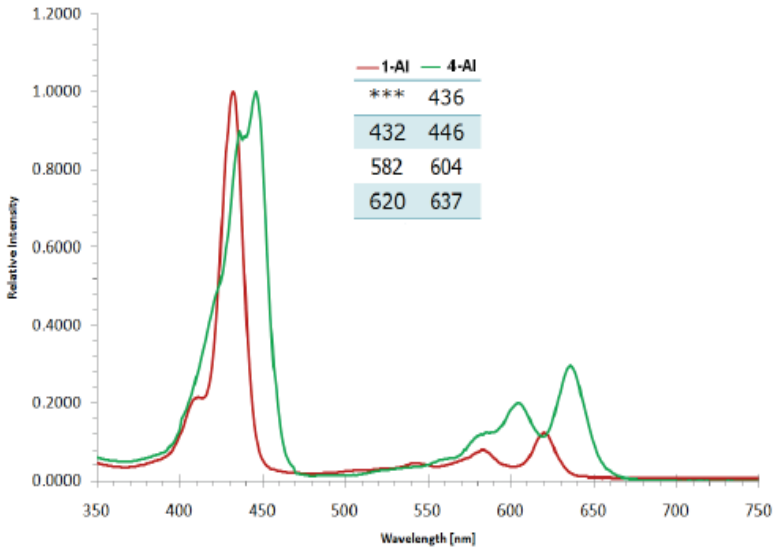

Figure 7

Table 2: S_1 excitation energy (nm) and oscillator strength in pyridine at TDDFT/DFT/PBE0/SV(P) level of theory

	1 Al	4 Al	1 Ga	4 Ga	1 Ir	4 Ir	1 fb	4 fb
λ_{max}	545	569	544	567	521	532	521	547
f	0.1081	0.1962	0.1246	0.2103	0.0277	0.2205	0.0999	0.3390
Exp.	620	637	594[5]		620[6]			

To evaluate the ability to excite to oxygen to the triplet state we calculate the triple t energy reported on table 3. All the compounds have a n E_T greater than 0.98 eV, what make them able to be used on PDT.

Table 3: T_1 excitation energy (eV) in pyridine at TDDFT/DFT/PBE0/SV(P) level of theory

	1 Al	4 Al	1 Ga	4 Ga	1 Ir	4 Ir	1 fb	4 fb
E	1.34	1.21	1.34	1.21	1.43	1.33	1.25	1.06

Bibliography

[1]Simkhovich, L; Goldberg, I; Gross, Z (2000)
First syntheses and X-ray structures of a meso-alkyl-substituted corrole and its Ga(III) complex
Journal of Inorganic Biochemistry, Vol 80, Issue 3-4, 235-238

[2]Bendix J, Dmochowski IJ, Gray, HB et al.(2000)
Structural, electrochemical, and photophysical properties of gallium(III) 5,10,15-tris(pentafluoro-phenyl)corrole
ANGEWANDTE Chemie International Edition, Vol 39, Issue 22, 4048-4051

[3] Mahammed, A; Goldberg, I; Gross, Z (2001)
Highly selective chlorosulfonation of tris(pentafluorophenyl)corrole as a synthetic tool for the preparation of amphiphilic corroles and metal complexes of planar chirality
Organic Letters, Vol 3, Issue 22, 3443-3446

[4]Vestfrid, Jenya; Botoshansky, Mark; Palmer, Joshua H.; et al.(2011)
Iodinated Aluminum(III) Corroles with Long-Lived Triplet Excited States
Journal of the American Chemical Society, Vol 133, Issue 33, 12899-12901

[5] Sorasaenee, Karn; Taqavi, Pouyan; Henling, Lawrence M.; et al (2007)
Amphiphilic aluminium(III) and gallium(III) corroles
Journal of Porphyrins and Phthalocyanines, Vol 11, Issue 3-4, 189-197

[6]Palmer, Joshua H.; Durrell, Alec C.; Gross, Zeev; et al.(2010)
Near-IR Phosphorescence of Iridium(III) Corroles at Ambient Temperature
Journal of the American Chemical Society, Vol 132, Issue 27, 9230-9231